Contrib Mineral Petrol (1998) 132: 269–287

Daniela Rubatto · Dieter Gebauer · Mark Fanning

Jurassic formation and Eocene subduction of the Zermatt–Saas-Fee ophiolites: implications for the geodynamic evolution of the Central and Western Alps

Received: 1 December 1997 / Accepted: 8 April 1998

Abstract The Zermatt–Saas-Fee ophiolites (ZSFO) are one of the best preserved slices of eclogitic oceanic crust in the Alpine chain. They formed during the opening of the Mesozoic Tethys and underwent subduction to H*P*/UH*P* conditions during Alpine compression. A cathodoluminescence-based ion microprobe (SHRIMP) dating of different zircon domains from metagabbros and oceanic metasediments was carried out to constrain the timing of formation and subduction of this ophiolite, two fundamental questions in Alpine geodynamics. The formation of the ophiolitic sequence is constrained by the intrusion ages of the Mellichen and the Allalin metagabbros (164.0 ± 2.7 Ma and 163.5 ± 1.8 Ma) obtained on magmatic zircon domains. These data are in line with the maximum deposition age for Mn-rich metasediments which overlie the mafic rocks at Lago di Cignana (161 ± 11 Ma) and at Sparrenflue (ca. 153–154 Ma). An Eocene age of 44.1 ± 0.7 Ma was obtained for whole zircons and zircon rims from an UH*P* eclogite and two metasediments at Lago di Cignana. One of the Eocene zircons contains a rutile inclusion indicating formation at H*P* conditions. As the temperature and pressure peak of these rocks nearly coincide, the Eocene zircons probably constrain the age for the deepest subduction of the ZSFO. This Eocene age for the UH*P* metamorphism implies that the ZSFO were subducted later than the Adriatic margin (Sesia-Lanzo Zone) and before the Late Eocene subduction of the European continental crust below Apulia. A scenario with three subduction episodes propagating in time from SE to NW is proposed for the geological evolution of the Central and Western Alps.

D. Rubatto[1] · D. Gebauer
Institut für Isotopengeologie und Mineralische Rohstoffe, ETH-Zentrum, Sonneggstrasse 5, CH-8092, Zürich, Switzerland

M. Fanning
Research School of Earth Sciences, The Australian National University, Mills Road, Canberra ACT 0200, Australia

Present address:
[1]Research School of Earth Sciences, The Australian National University, Mills Road, Canberra ACT 0200, Australia
e-mail: Daniela.Rubatto@anu.edu.au

Editorial responsibility: J. Hoefs

1 Introduction

The Alpine chain was formed by collision of the European plate with the Adriatic plate during the Cretaceous and Tertiary (e.g. Laubscher and Bernoulli 1982; Polino et al. 1990; Stampfli and Marchant 1997). The convergence between these two continents led to subduction of oceanic and continental crust under the Adriatic margin. In the Central and Western Alps, remnants of at least two oceanic basins are preserved: the Piemontese–Ligurian ocean and the Valais trough. The Piemontese–Ligurian ocean represents the Mesozoic Tethys, an ocean basin that developed between Europe and Africa, following Triassic to Jurassic extension and rifting in relation to the opening of the Central Atlantic (e.g. Stampfli 1996). The Valais trough was a smaller basin located NW of the Tethys, which formed in the Late Jurassic–Early Cretaceous, simultaneously to the opening of the North Atlantic (e.g. Stampfli and Marchant 1997).

The Zermatt–Saas-Fee ophiolites (ZSFO) are a dismembered ophiolitic sequence (e.g. Bearth 1967; Meyer 1983; Barnicoat and Fry 1986; Bowtell 1991) that represent the Piemontese–Ligurian ocean. During Alpine convergence these ophiolites were subducted to high-pressure (H*P*) and ultra-high-pressure (UH*P*) conditions and they partly preserve the eclogitic parageneses. Therefore, the geology of the ZSFO is fundamental for the understanding of the Jurassic opening and the Alpine closure of the Tethys ocean.

In spite of the relatively well constrained metamorphic and magmatic evolution, geochronological data on both timing of ophiolites formation and of Alpine metamorphism are either not available or inconclusive. The K-Ar or Rb-Sr age determinations (e.g. Bocquet et al. 1974; Hunziker 1974; Delaloye and Desmons 1976), largely used in past years, have not been able

precisely to date protolith formation and Alpine subduction. Conventional U-Pb dating has also been unsuccessful because of the extremely low U-contents of zircons in most of the mafic rocks of this area (S.M. Reddy, personal communication and this work).

Samples from different localities and rock types were studied combining both cathodoluminescence (CL) investigations and U-Pb dating of zircon using the sensitive high resolution ion microprobe (SHRIMP) at the ANU in Canberra. The aims of this work were: (1) to determine the age of magmatic emplacement of two major gabbro bodies and to obtain a maximum depositional age of the overlying oceanic sediments in order to constrain in time the formation of the ophiolites; (2) to provide constraints on the timing of subduction of the ZSFO by dating the Alpine H*P* and UH*P* metamorphism. The comparison between our results and other recent age determinations indicated that the Alpine subduction was poly-episodic and migrated in time from SE to NW of the Alpine chain. It is demonstrated that the ZSFO were subducted while other eclogitic nappes were either partially exhumed or not yet involved in the collision.

2 Geological setting

2.1 The Zermatt–Saas-Fee ophiolites

The studied area (Fig. 1) is located in the inner Alpine belt (Pennine domain), between the units derived from the Adriatic margin (Sesia-Lanzo Zone and Austroalpine domain) and the Briançonnais continental block, which separated the Piemontese–Ligurian ocean from the Valais trough (see also Fig. 14). In this area the Mesozoic Tethyan ocean is represented by the ZSFO and the overlying Combin unit s.s. (Tsaté nappe; Sartori 1987).

The Combin unit s.s. (Bearth 1967; Dal Piaz et al. 1979) or Tsaté nappe (Sartori 1987) consists of a pre-ophiolitic basal complex (Dal Piaz et al. 1979) and an overlying ophiolite-bearing sequence with continental affinity mainly composed of calcschists, marbles, quartzitic schists and metabasic rocks (Dal Piaz et al. 1979; Sartori 1987). It has been interpreted to represent a sequence deposited on a thinned continental margin (Dal Piaz et al. 1979) or an accretionary prism (Marthaler and Stampfli 1989). This unit displays a pervasive epidote/blueschist-facies metamorphism lacking eclogitic assemblages that, by contrast, are well documented in the underlying ZSFO. The main rock types of the ZSFO were first comprehensively described by Bearth (1967). The ZSFO are mainly composed of metagabbros with relic magmatic textures (Allalin and Mellichen, Fig. 1; e.g. Meyer 1983) and metabasalts, which locally still preserve pillow lava structures (e.g. at Pfulwe, Fig. 1; Barnicoat and Fry 1986). Basaltic dikes within metagabbros have been interpreted by some authors (Barnicoat and Fry 1986; Bowtell 1991) as a reduced sheeted dike complex (e.g. at Mellichen, Fig. 1). Serpentinized ultrabasic rocks occur as large lenses within the mafic rocks (e.g. Bearth 1967; Meyer 1983). The metabasalts are directly overlain by metapelites, marbles and Mn-bearing quartzites (at Sparrenflue, Mittaghorn, Lago di Cignana and Plan Maison), which form a thin cover of the oceanic crust (Dal Piaz et al. 1979; Bearth and Schwander 1981).

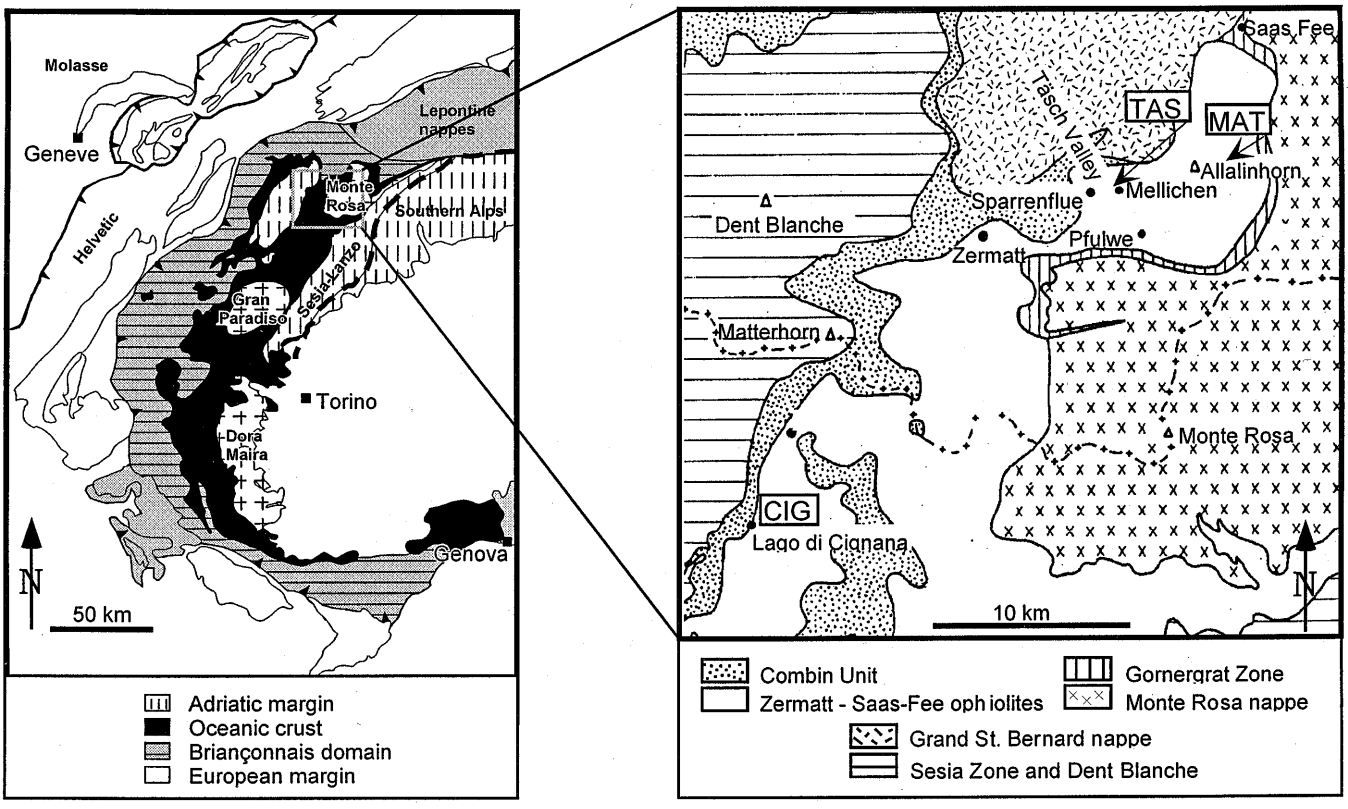

Fig. 1 **a** Simplified geological map of the Western Alps with the location of the area studied. **b** Geological map of the Zermatt-Saas-Fee area after Barnicoat and Fry (1986). The *initials* indicate the three localities investigated. (*MAT* Mattmark dam where the Allalin samples were collected, *TAS* Täsch Valley, *CIG* Lago di Cignana)

2.2 The sample localities

Within the ZSFO three main areas have been studied (Fig. 1): the area of the Allalin metagabbro, the Täsch Valley (Mellichen metagabbro and Sparrenflue metasediments) and the Lago di Cignana (LdC) region. In all these localities the parageneses of the Alpine H*P* or UH*P* metamorphism are preserved and the metamorphic evolution as well as the *P-T* paths are well established (Meyer 1983; Barnicoat and Fry 1986; Reinecke 1995). These are favourable conditions for a detailed isotopic investigation.

The eclogite-facies Allalin metagabbro forms the largest metagabbro body in the ZSFO. It is one of the best examples of preserved igneous textures, structures and mineralogy in the ZSFO (Meyer 1983).

In the Täsch Valley (Fig. 2) the metabasalts are the main rock types with different degrees of metamorphic overprint, from eclogite- to greenschist-facies conditions (e.g. Barnicoat and Fry 1986; Bowtell 1991). The metagabbros occur as elongated lenses within the metabasalts with a major body in the Mellichen area.

The oceanic metasediments form a nearly continuous layer at the top of the ZSFO (Bearth and Schwander 1981). In the studied area they are represented by Mn-bearing metasediments directly overlying the metabasalts. At Sparrenflue, the metasediments are in stratigraphic contact with the metabasalts and form a few metres thick, continuous cover comprising quartz-rich Mn-micaschists and Mn-rich massive metaquartzites. At LdC, the mafic rocks and the metasediments form a tectonic melange (Reinecke 1991). This unit (Fig. 3) consists of a layer of garnet + ankerite-bearing micaschists with interbedded lenses of retrogressed eclogites and omphacite-rich eclogites, which overlies more or less retrogressed eclogites (Bearth 1967). The latter are interpreted as metabasalts because they preserve relics of former pillows (Reinecke et al. 1994). Manganese-metaquartzites occur as a few metre thick intercalations within the micaschists.

2.3 Metamorphic evolution

The geological history of the ZSFO evolved through four main stages summarised below (for metamorphic assemblages see Table 1).

1. Formation of the ophiolitic sequence with crystallisation of gabbros and basalts during the opening of the ocean basin and deposition of sediments in an oceanic environment.

2. The (U-)H*P* metamorphism during Alpine compression. The prograde path is recorded within the garnets of the Cignana metasediments (Reinecke 1995; van der Klauw et al. 1997) and partly in the Allalin metagabbro (Meyer 1983). The maximum temperatures are around 600 °C in all three localities, while the estimated pressures are higher at LdC where the presence of coesite (Reinecke 1991) indicates a pressure of 28–30 kbar (Table 1). From the rest of the ZSFO pressures of ~20 kbar are reported (Meyer 1983; Barnicoat and Fry 1986). However, higher pressures (35 kbar) have also been proposed for the Allalin gabbro (Barnicoat 1996).

3. Blueschist-facies overprint. This stage was characterised by a significant decompression accompanied by cooling (100–50 °C; Table 1).

4. Greenschist-facies overprint that was marked by strong decompression to 4–5 kbar and cooling under 500 °C (Table 1).

In conclusion, the metamorphic evolution of the three localities was similar. However, subduction to greater depth is recorded in the LdC sequence, which cannot totally be excluded for the other parts of the ZSFO, at least for the Allalin metagabbro (Barnicoat 1996).

3 Sample description

This section concentrates on the description of the mineral assemblages and textures that were observed in the samples analysed

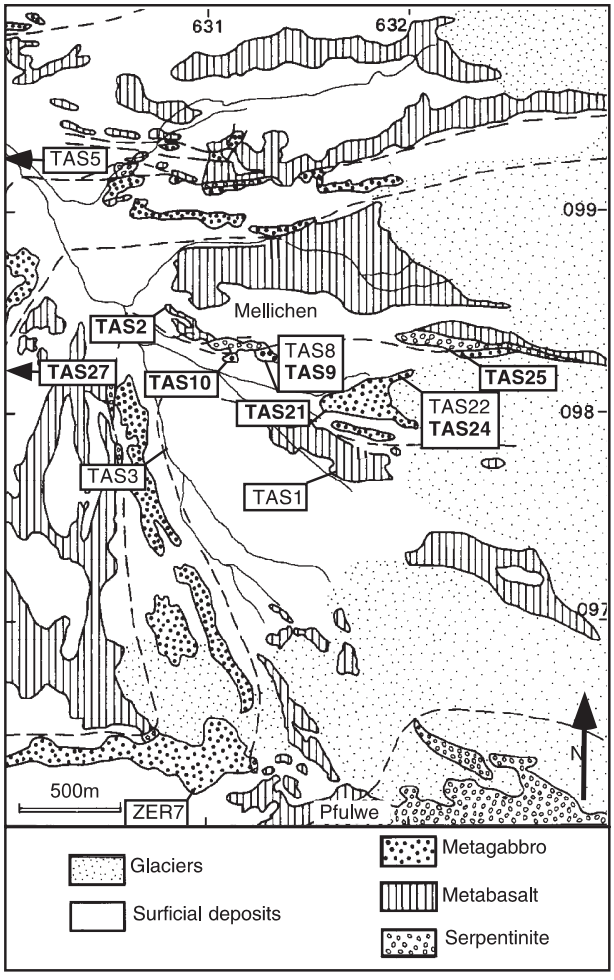

Fig. 2 Sample location in the upper Täsch Valley. The lithological map is based on unpublished data of B.J. Davidson and R.P. Metcalfe and redrawn after Fry and Barnicoat (1987). Samples TAS5 and TAS27 are located a few hundreds of metres *outside* the map in the direction indicated. The samples dated are indicated *in bold*

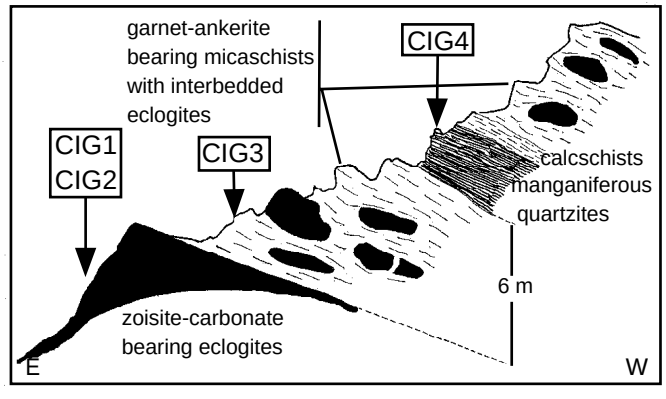

Fig. 3 Geological profile of the Lago di Cignana sequence, with sample locations (redrawn after Bearth 1967)

Table 1 Metamorphic evolution of the three studied localities. Mineral abbreviations according to Bucher and Frey (1994)

Locality and data-source	Main rock type	Stage 2: H*P*/UH*P* metamorphism		Stage 3: blueschist facies (decompression and cooling)		Stage 4: greenschist facies	
		Assemblage	*P–T*	Assemblage	*P–T*	Assemblage	*P–T*
Allalin	metagabbro[a]	1) Opx-gt-ompI-zo--jd-qtz-kyI-rt	18–20 kbar 650–725 °C	1) GlnI-omIII-tcII--pgI-phe-ctd-qtz	19–14 kbar 480–550 °C	Ab-zo-czo-hbl-chl--pgIII-marII-bt-rt-tnt	4 kbar? 500 °C
(Meyer, 1983)		2) OmpII-tc-kyII-ctd-zo-qtz-rt	> 20 kbar 550–600 °C	2) Olig-czo-glnII--hblI-chlI-pgII--marI-crn-ilm-hem	14–4 kbar ca. 500 °C		
Täsch Valley	Eclogite	1) OmpI-gtI-czo-ky--tc-qtz-rt	17–20 kbar 550–600 °C	Gln-ompII-gtII-czo--pg-qtz-rt	< 15 kbar ≤550 °C	Na-am–Ca am-ab	< 10 kbar ≤550 °C
(Fry and Barnicoat, 1987)		2) Lws-gtI-ompI	< 17–20 kbar < 600 °C				
Lago di Cignana (Reinecke 1991, 1995; Reinecke et al. 1994; van der Klauw et al. 1997)	Eclogite	Gt-omp-gln-cs-phe--czo-rt-py-dol	28–30 kbar 580–630 °C	Blue/green am-ab	≤12–13 kbar ≤550 °C	Ca/Na am-ab-chl--ep-tnt	5 kbar 400 °C
	Metasediments	1) GtI-phe-cs-ep-jd--gln-rt-ap-arg-hem	28–30 kbar 580–630 °C			GtIII-ab-cal-chlII--pheIII-phl-tr-hem–kfs-qtz	< 16 kbar < 500 °C
		2) Qtz-gtII-dol-arg--chlI-lws- pheII-rt-aln	17–19 kbar 500–540 °C				

[a] Metagabbro with magmatic relics of ol-pl-chr

in order to locate them within the metamorphic evolution described above. The samples are listed according to locality and rock type. Assemblages are listed in Table 2.

3.1 The metagabbros

Four samples of the Allalin metagabbro were collected close to the Mattmark dam. Sample MAT2 is an olivine-metagabbro that preserves its magmatic texture and contains pseudomorphs after igneous olivine and clinopyroxene. The eclogitic assemblage is largely preserved. Sample MAT6 is the product of H*P* metamorphic transformation of an olivine-gabbro partly retrogressed into albite-amphibole symplectite. Despite its deformation, structural relics of olivine transformed into talc + garnet ± rutile are still visible. A mafic dike with an eclogitic paragenesis and a coarse grained metagabbro were also sampled in that area, but no zircons were recovered from these samples.

In the Täsch Valley metagabbros, metabasalts, a carbonate-rich vein and a retrograde albite-rich vein were collected (Fig. 2). The leucogabbros from the Mellichen area (TAS9, 10, 21, and 24), which occur as bands or pods within coarse-grained gabbros, were the most suitable for dating. They contain zircons probably because of the high degree of differentiation. The samples dated show various grades of retrogression and deformation of the H*P* paragenesis (Table 2). Sample TAS21 partially preserves the H*P* assemblage with spectacular albite-amphibole symplectites after omphacite. The coarse-grained magmatic texture can be recognised because of the preservation of pseudomorphs after plagioclase (zoisite + white mica ± albite) and after clinopyroxene (albite + amphibole). Sample TAS9 is more strongly deformed and the only relic of the H*P* assemblage is garnet. Samples TAS10 and TAS24 are completely retrogressed under greenschist-facies conditions. Sample TAS10 is a Mg-rich leucogabbro with pseudomorphs after Mg-chloritoid and TAS24 is a relatively quartz rich metagabbro. A zoisite-quartz greenschist-facies vein collected within metabasic rocks (TAS2) contains exclusively pre-Jurassic zircons, which probably are derived from the county rock, as commonly observed in metamorphic veins (Rubatto 1998). No zircons were found in a meta-pillow basalt (TAS1), a carbonate-rich level within eclogite (TAS5) and a retrogressed metagabbro (TAS3). Zircons from a metagabbro from Pfulwe (ZER7) could not be analysed because of the extremely low U-concentrations (< 1 ppm).

3.2 The eclogites at Lago di Cignana

In this locality two samples of the eclogites (CIG1 and CIG2) that are directly overlain by micaschists were collected (Fig. 3). Sample CIG1 is a massive eclogite with a fresh H*P* assemblage consisting of large poikiloblastic garnets surrounded by a fine matrix of omphacite + phengite + glaucophane ± rutile. A stronger foliation and re-equilibration at lower pressures characterise the eclogite CIG 2 that still preserves the peak paragenesis partly overprinted by a glaucophane-rich assemblage.

3.3 The metasediments

The sample TAS27 is a metasediment cropping out at Sparrenflue (Fig. 2). It is a fine-grained metaquartzite consisting of centimetre-thick layers of quartz + mica ± spessartine ± piemontite ± Mn-oxides alternating with layers richer in Mn-minerals and poorer in quartz. In these layers spessartine and piemontite are more abundant, while the micas are pink in colour indicating enrichment in Mn. Millimetre-sized nodules of Mn-oxides and spessartine can be observed.

In the area of LdC two different metaquartzites were collected (Fig. 3). Sample CIG3 is a quartzitic layer (ca. 70% quartz) that contains porphyroblasts of garnet (spessartine) full of inclusions of quartz, phengite and hematite. Smaller garnets are also present in the matrix together with red piemontite, which overgrows the schistosity. The sample CIG4 is a metaquartzite richer in Mn as

Table 2 Metamorphic assemblages of the samples dated. The white mica composition was estimated petrographically based on the equilibrium paragenesis. On the other hand, the initial *wm* indicates white mica of unknown composition. H*P* minerals given in *brackets* are not preserved, but their structural relics and pseudomorphs are clearly seen. The last two columns indicate the number of zircons analysed and the number of total SHRIMP analyses for each sample. Mineral abbreviations according to Bucher and Frey (1994)

Sample	Rock type	Locality	H*P* mineral assemblage	Retrograde assemblage	N. zircons analysed	N. spots
MAT2	Metagabbro	Allalin Glacier	Pg-gt-tc-rt ± ky[a]	Zo-wm	8	14
MAT6	Metagabbro	Allalin Glacier	ZoI-pg-gt-omp-tc-rt[b]	ZoII-ab-wm	4	5
TAS2	Low grade vein	Mellichen		Qtz-zo-ms-cal-ab-ep	3	4
TAS9	Leucogabbro	Mellichen	Gt-rt-pgI-(omp)	PgII-czo-ab-amp-chl (symplectite after omp)	6	15
TAS10	Leucogabbro	Mellichen	Rt-(ctd)	Amp-pg-czo-ab-rt-tnt-tc	6	7
TAS21	Leucogabbro	Mellichen	Gt-pgI-qtz-(omp)	Qtz-pgII-zo-ab-amp-tnt (symplectite after omp)	5	7
TAS24	Leucogabbro	Mellichen	(Omp-gt)	Qtz-zo-amp-pg-ab (symplectite after omp)	4	8
TAS25	Metagabbro	Mellichen	Omp-gt-pg	Ab	4	4
TAS27	Metasediment	Täsch Valley	Qtz-phe-gt-ep-oxides		7	7
CIG1	Eclogite	Lago di Cignana	Gt-omp-rt-gln-phe	Amp-chl-qtz	3	5
CIG2	Eclogite	Lago di Cignana	Gt-omp-gln-czo-rt	Tnt-chl	3	3
CIG3	Metasediment	Lago di Cignana	Qtz-phe-gt-ep-hem-rt	Chl-bt-kfs	9	18
CIG4	Metasediment	Lago di Cignana	Qtz-gt-ank-ep-phe-hem		3	3
total					65	100

[a] Presence of pseudomorphs replacing igneous minerals (ol-pl-cpx)
[b] Presence of pseudomorphs after igneous olivine

documented by the abundance of spessartine and piemontite as well as the presence of ankerite.

Coesite or quartz after coesite, as it was previously described by Reinecke (1991) and Reinecke et al. (1994), were not observed in our samples from LdC.

4 Methods

All samples were crushed and sieved to less than 320 μm. Zircons were separated according to magnetic properties and density and finally selected by hand picking. They were sorted into fractions according to shape, colour and dimension, embedded in epoxy and polished down to half sections. The same mount was used for CL imaging and SHRIMP analyses. The selection of zircons for SHRIMP analyses was done on the basis of the CL images.

The zircons were analysed for U, Th and Pb using the sensitive high resolution ion microprobes (SHRIMP I and II) at the Australian National University in Canberra. Instrumental conditions and data acquisition were generally as described by Compston et al. (1992). As reference, zircons from a pegmatite from Sri Lanka (SL13) were used in 1995 and 1996, while in 1997 zircons from a gabbro of the Duluth Complex in Minnesota (AS3) were used in addition to the SL13 zircons. The data were treated following Compston et al. (1992) and plotted in the classical concordia diagram or in the Tera–Wasserburg diagram (TW) introduced by Tera and Wasserburg (1972). For the TW diagrams data uncorrected for common lead have been used. The mean ages are weighted means at the 95% confidence level, while the single data points listed in Tables 3, 4, 5, 6 and 7 are given with 1 sigma errors.

The single zircon used for conventional U-Pb analyses was air-abraded, washed in warm 4 N nitric acid, and rinsed several times with distilled water and acetone in an ultrasonic bath. Dissolution and chemical extraction of U and Pb were performed following Krogh (1973) using bombs and anion exchange columns scaled down to 1/10 of their original size. Total procedural blanks were 2 pg Pb and 0.1 pg U. A mixed ^{205}Pb-^{235}U tracer solution was used for the analyses. The Pb and U were loaded together on a single Re filament with Si-gel and phosphoric acid and measured on a Finnigan MAT 262 mass spectrometer using an ion counting system.

The CL investigation was carried out on a CamScan 4 scanning electron microscope (SEM) at the Institut für Metallforschung und Metallurgie at the ETH in Zürich. The instrument is supplied with an ellipsoidal mirror for CL (e.g. Gebauer 1996). Panchromatic CL and secondary electron pictures were taken with 1 minute scanning time on black and white films. Operating conditions for the SEM were 13 kV and current of ~120 μA.

Cathodoluminescence is a crucial tool for SHRIMP dating because it enables (1) identification of zircon areas relatively richer in U; (2) recognition of different types of zircon domains on the basis of their zoning patterns. There is a qualitative negative correlation between CL intensity and U-content (e.g. Rubatto and Gebauer in press): bright areas in CL are generally U poor compared to darker areas. The identification of U-rich areas was particularly useful for some of the relatively young and U-poor zircons discussed in this work because analyses of such areas resulted in more precise SHRIMP U-Pb data. The identification of CL domains characterised by different zoning pattern is fundamental for SHRIMP analysis in order to avoid the phenomenon of mixed ages.

5 Geochronological results

5.1 The Allalin metagabbro

The olivine-gabbro MAT2 contains a relatively homogeneous zircon population. The CL images (Fig. 4) suggest that the zoning bands grew freely forming euhedral crystals that were subsequently broken and partially resorbed. Micro-fractures sealed with a bright luminescing product are also evident in the CL images; they are probably responsible for the radiogenic lead

loss. Within this homogeneous population no traces of inherited cores were observed. Only one zircon had an irregularly zoned rim, characterised by strong CL emission, which was large enough to be dated (MAT2-2.2). Eight data points obtained from oscillatory-zoned domains, commonly interpreted as magmatic (e.g. Schärer et al. 1995; Vavra et al. 1996; Gebauer 1996; Rubatto and Gebauer in press), yielded Middle Jurassic ages and lie on a simple mixing line with common lead (Fig. 5) with a lower intercept at 164.0 ± 2.7 Ma. These analyses correspond to domains with U-contents above 279 ppm and Th/U ratios higher than 0.2 (Table 3), as typical for magmatic zircons (Rubatto and Gebauer in press). One data point that plots to the right of the mixing line corresponds to the light rim (MAT2-2.2).

Two zircons that show rounded shapes and a CL zoning different from that of the main zircon population, yielded Carboniferous ages (MAT2-1 and MAT2-7; Table 7). The second sample, the olivine-gabbro MAT6, does not contain a uniform zircon population, but zircons with various shapes ranging from rounded to broken and different types of oscillatory zoning. Zircons from this sample yielded $^{207}Pb/^{206}Pb$ ages ranging between 1.7 and 2.8 Ga (see section 5.5.).

5.2 The Mellichen metagabbro

The leucogabbros collected within the Mellichen metagabbro (TAS9, 10, 21 and 24) contain similar zircon populations: most of the grains do not preserve planar crystal faces, but have irregular surfaces. The zircons are not transparent in transmitted light and are light pink or yellow to brown in colour. In CL (Fig. 6) the irregular surfaces of the zircons are even more evident: they show embayments, micro-fractures and inclusions. Only restricted zircon domains still preserve a magmatic zoning with oscillating zones grown parallel to previous euhedral faces. Cloudy-zoned or unzoned areas are present around inclusions or in peripheral locations. In CL no inherited cores were identified.

Most of the U-Pb analyses of oscillatory domains and some analyses of cloudy-zoned or unzoned areas/rims yielded Middle–Late Jurassic ages (Table 4). These data cluster on a common Pb mixing line in the TW diagram (Fig. 7). The mean ages for each of the four samples are indistinguishable: TAS9 yielded an age of 163.6 ± 3.5 Ma, TAS10 an age of 162.4 ± 3.5 Ma and TAS21 an age of 164.1 ± 5.3 Ma. On sample TAS24 only two spots yielded an age around 165–167 Ma. As all these samples were collected in the same area and represent the same rock type it is plausible to calculate a pooled mean for all the data points, giving an age of 163.5 ± 1.8 Ma.

Conventional isotope dilution U-Pb dating was carried out on one single zircon from the leucogabbro TAS21. The analysis is concordant (Fig. 8) and yields a $^{206}Pb/^{238}U$ age of 164.1 ± 0.7 Ma, which is in agreement with the SHRIMP results. Conventional dating was attempted also for a metagabbro from Pfulwe (ZER7) that contain zircons with U-contents below the detection limit of SHRIMP. Because of the low total Pb-content (0.24 ppm) and the high proportion of common Pb, no age could be calculated.

Younger SHRIMP U-Pb ages were also obtained, but these analyses do not form a unique cluster or clusters on the TW plot and, therefore, are interpreted as not representing geologically significant event(s). The analyses yielded apparent ages from Jurassic to Eocene (Table 4). None of these analyses were carried out on oscillatory-zoned domains, apart from two analyses in sample TAS9 where micro-fractures are clearly visible in CL image (Fig. 6). The sample TAS25, a H*P* metagabbro with a

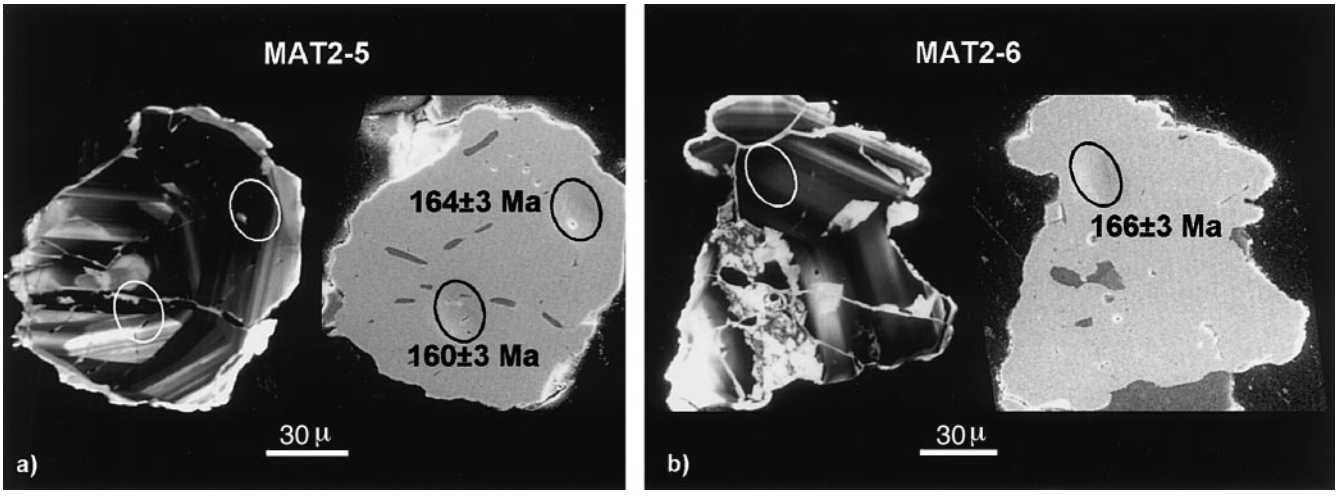

Fig. 4a, b Zircons from the Allalin metagabbro: secondary electron images (on the *right*) and panchromatic CL images (on the *left*). **a** Zircon MAT2-6; **b** Zircon MAT2-5. Note the irregular shape, the magmatic zoning parallel to previous crystal faces and the microfractures sealed by a highly luminescing product

preserved magmatic texture, contained only few zircons, most of them with U- and Pb-contents below the detection limits of SHRIMP. The only two spots dated plot to the right of the cluster defined by the other samples.

5.3 The metasediments in the Täsch Valley

The Mn-rich metaquartzite of the Täsch Valley (TAS27) contains an extraordinarily high amount of zircons for a sediment deposited in deep oceanic environment (several hundreds of zircons out of ca. 2 kg of rock) where no detrital components are expected. The same observation is valid for the sediments dated at LdC. In both cases the source of the zircons needs to be understood in order to constrain the deposition of the sediment and the evolution of the oceanic basin.

The zircons separated from this sample show typologies uncommon for detrital minerals. They are not rounded as would be expected for detrital minerals that have been transported over long distances, but often have sharp edges and some of them even preserve their original euhedral shapes. In transmitted light no cores are visible and this observation is confirmed with CL investigation. The internal zonation shown in CL is rather simple (Fig. 9): the zircons are mainly uniformly oscillatory zoned, and have an irregular thin rim (less than 10 μm) of possibly Alpine metamorphic origin. Shape, oscillatory zoning, U-contents and Th/U ratios of these zircons are very similar to the zircons from the metagabbros (see Tables 3 and 4).

The ages obtained are all Middle to Late Jurassic, ranging between 153 and 173 Ma (Table 5; see section 6.2 for discussion).

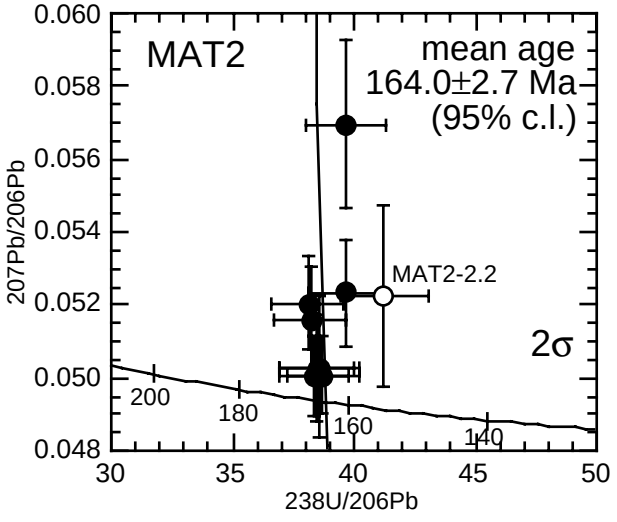

Fig. 5 Allalin metagabbro MAT2: TW diagram. The point MAT2-2.2 was not considered in drawing the correlation line and in calculating the age. Only the Jurassic ages are reported; the inherited components are shown in Fig. 13

Table 3 Allalin metagabbro MAT2: U, Th and Pb SHRIMP data. Pre-Jurassic ages and data from sample MAT6 are reported in Table 7 (* are the data yielding the intrusion age)

Spot name	U (ppm)	Th (ppm)	Th/U	Pb radiogenic (ppm)	% Common Pb	207/206 uncorrected	±207/206	238/206 uncorrected	±238/206	206/238	±206/238	Age (Ma) 206/238	±	CL domain
*MAT2-2.1	279	254	0.91	8	0.80	0.0570	0.0010	39.7	0.8	0.0250	0.0005	159	3	Oscillatory
*MAT2-3.1	659	810	1.2	21	0.30	0.0521	0.0006	38.1	0.7	0.0262	0.0005	166	3	Oscillatory
*MAT2-4.1	625	152	0.20	16	0.10	0.0503	0.0007	38.5	0.8	0.0260	0.0005	165	3	Oscillatory
*MAT2-5.1	533	1433	2.7	22	0.30	0.0523	0.0007	39.7	0.8	0.0251	0.0005	160	3	Oscillatory
*MAT2-6.1	940	1155	1.2	30	0.10	0.0500	0.0006	38.3	0.7	0.0261	0.0005	166	3	Oscillatory
*MAT2-8.1	496	645	1.3	16	0.20	0.0516	0.0007	38.2	0.8	0.0261	0.0005	166	3	Oscillatory
*MAT2-3.2	574	453	0.78	16	0.10	0.0500	0.0010	38.6	0.8	0.0259	0.0006	165	3	Oscillatory
*MAT2-5.2	940	1820	1.9	35	0.08	0.0501	0.0005	38.7	0.8	0.0258	0.0005	164	3	Oscillatory
MAT2-2.2	192	104	0.54	5	0.30	0.0520	0.0010	41.2	0.9	0.0242	0.0005	154	3	Light rim

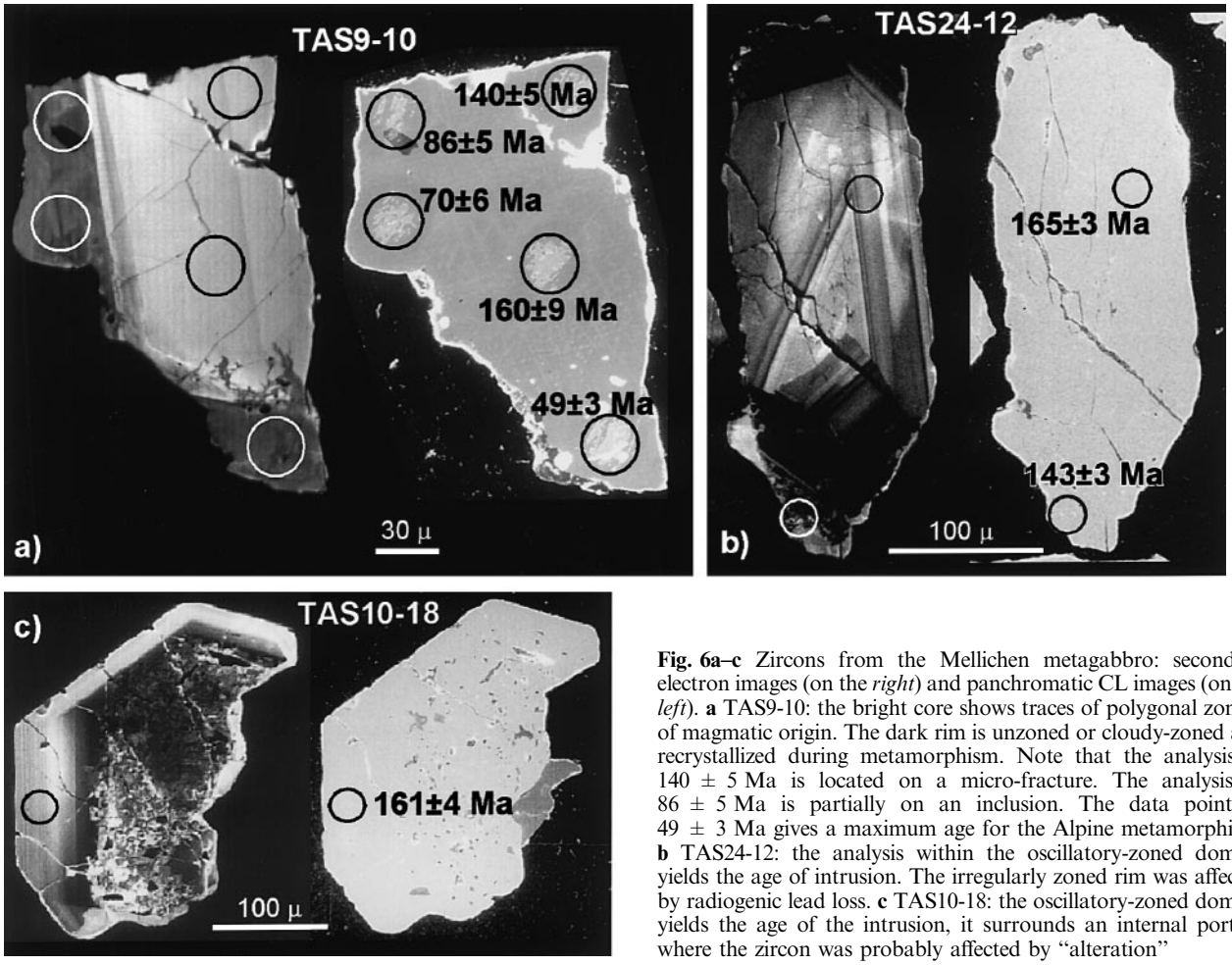

Fig. 6a–c Zircons from the Mellichen metagabbro: secondary electron images (on the *right*) and panchromatic CL images (on the *left*). **a** TAS9-10: the bright core shows traces of polygonal zoning of magmatic origin. The dark rim is unzoned or cloudy-zoned and recrystallized during metamorphism. Note that the analysis at 140 ± 5 Ma is located on a micro-fracture. The analysis at 86 ± 5 Ma is partially on an inclusion. The data point at 49 ± 3 Ma gives a maximum age for the Alpine metamorphism. **b** TAS24-12: the analysis within the oscillatory-zoned domain yields the age of intrusion. The irregularly zoned rim was affected by radiogenic lead loss. **c** TAS10-18: the oscillatory-zoned domain yields the age of the intrusion, it surrounds an internal portion where the zircon was probably affected by "alteration"

5.4 Metasediments and eclogites from Lago di Cignana

An Alpine age was obtained in zircons from an eclogite (GIG2) and two metasediments (CIG3 and CIG4) from LdC. Only three zircons could be separated from the eclogite CIG2: they are clear, transparent and between 100 and 200 μm in length. The metasediment CIG4 also contained only few zircons, which are clear and much smaller in size (< 50 μm). The metasediment CIG3 was relatively richer in zircons with different sizes (from < 100 μm to several hundreds of μm), shapes and colours. The zircons from CIG2 and CIG4 show a rather regular CL zoning characterised by oscillatory bands or sectors (Fig. 10). A rutile inclusion in a zircon from the metasediment CIG2 has been detected by Raman spectroscopy (Fig. 10b). The zircon population of the metasediments CIG3 is more heterogeneous also in CL. Most of the crystals show clear cores, generally with oscillatory zoning, surrounded by rims with different zoning patterns.

The zircons that could be dated from both the eclogite CIG2 and the metaquartzite CIG4 (some zircons of CIG4 were too low in U) yielded a Middle Eocene age, independent of their zonation patterns (Table 6 and Fig. 11). In the metasediment CIG3 a similar Alpine age was obtained in different zircon domains. The Alpine age recorded in the eclogite is 44.5 ± 2.3 Ma (3 data points), while the two samples of metasediments carry zircons entirely or partially formed 43.9 ± 0.9 Ma ago (12 data points). As the ages from both rock types are within uncertainty of each other, a mean age of 44.1 ± 0.7 Ma can be calculated. No indications of younger lead loss were detected.

Pre-Alpine ages ranging from Precambrian to Jurassic were obtained from zircon cores of the metasediment CIG3 (Table 6) indicating a detrital origin for these zircon cores. The youngest zircon core, which displays magmatic zoning, was dated at 161 ± 11 Ma with three concordant data points (Fig. 12). The eclogite CIG1 had only inherited zircons of various ages and those are discussed in section 5.5.

5.5 Inherited components and lead loss in zircons from the mafic rocks

The magmatic zircons within the mafic rocks in the ZSFO yield an age around 164 Ma and therefore all the zircons or zircon cores yielding a pre-Jurassic age are considered to be inherited. In many of the mafic rocks

Table 4 Mellichen metagabbro (samples TAS9, TAS10, TAS21, TAS24 and TAS25): U, Th and Pb SHRIMP data (* are the data points considered for calculation of the Jurassic protolith age). When the CL zonation pattern is given in *brackets* the zoning is not well defined. "Altered" domains look like the core of the zircon in Fig. 6c

Spot name	U (ppm)	Th (ppm)	Th/U	Pb radioganic (ppm)	% Common Pb	207/206 uncorrected	±207/206	238/206 uncorrected	± 238/206	206/238	±206/238	Age (Ma) 206/238	±	CL domain
*TAS9-7.1	482	1188	2.47	20	1.2	0.0610	0.0010	37.9	0.8	0.0261	0.0005	166	3	(Oscillatory)
*TAS9-7.2	92	80	0.87	3	5.5	0.0990	0.0040	36.0	1.0	0.0260	0.0008	165	5	(Oscillatory)
*TAS9-1.1	335	643	1.92	12	1.3	0.0610	0.0020	39.0	1.0	0.0255	0.0007	163	4	(Oscillatory)
*TAS9-2.3	90	54	0.60	3	5.8	0.1030	0.0040	35.0	1.0	0.0270	0.0010	171	7	Cloudy
*TAS9-2.4	187	302	1.61	7	1.9	0.0660	0.0020	37.5	0.9	0.0262	0.0006	166	4	(Oscillatory)
*TAS9-10.1	30	474	15.6	4	26	0.2900	0.0200	30.0	2.0	0.0250	0.0010	160	9	(Oscillatory)
*TAS9-9.1	397	885	2.23	15	1.6	0.0640	0.0020	38.8	0.9	0.0254	0.0006	162	4	(Oscillatory)
*TAS9-9.2	597	1760	2.95	26	1.0	0.0590	0.0010	39.3	0.8	0.0252	0.0005	160	3	(Oscillatory)
TAS9-10.4	70	504	7.20	5	8.0	0.1220	0.0060	42.0	2.0	0.0220	0.0009	140	5	(Oscillatory)
TAS9-4.1	28	12	0.44	1	12	0.1600	0.0200	46.0	5.0	0.0190	0.0020	122	13	Oscillatory
TAS9-10.5	45	151	3.40	1	31	0.3300	0.0200	51.0	3.0	0.0134	0.0008	85.7	5.3	Cloudy rim
TAS9-10.2	28	<1	<0.01	<1	22	0.2500	0.0200	72.0	5.0	0.0109	0.0009	69.8	5.6	Cloudy rim
TAS9-10.3	55	4	0.01	<1	28	0.3000	0.0200	95.0	5.0	0.0076	0.0005	48.8	2.9	Cloudy rim
TAS9-2.1	5	<1	0.01	<1	52	0.5200	0.0800	77.0	11.0	0.0060	0.0010	40.3	9.2	Cloudy rim
*TAS10-20.1	1299	3396	2.61	52	0.30	0.0517	0.0007	39.1	0.7	0.0255	0.0005	162	3	Oscillatory
*TAS10-19.1	1177	2528	2.15	44	0.50	0.0540	0.0010	40.4	0.8	0.0247	0.0005	157	3	Oscillatory
*TAS10-18.1	196	261	1.34	6	4.2	0.0880	0.0020	37.8	0.9	0.0254	0.0006	161	4	Oscillatory
*TAS10-1.1	156	153	0.98	5	1.3	0.0610	0.0020	38.4	0.9	0.0257	0.0006	164	4	Unzoned
*TAS10-1.2	968	2148	2.22	38	0.16	0.0509	0.0005	38.1	0.7	0.0262	0.0005	167	3	Oscillatory
*TAS10-12.1	200	192	0.96	6	0.80	0.0560	0.0010	38.4	0.8	0.0259	0.0006	164	4	Cloudy rim
TAS10-13.1	265	274	1.04	8	0.90	0.0580	0.0010	41.2	0.9	0.0241	0.0005	153	3	Cloudy rim
*TAS21-38.1	182	154	0.85	6	0.90	0.0580	0.0020	37.0	1.0	0.0267	0.0007	170	5	Cloudy rim
*TAS21-34.1	49	44	0.90	1	4.3	0.0880	0.0050	39.0	2.0	0.0243	0.0009	155	6	Cloudy rim
*TAS21-46.2	214	163	0.76	6	0.80	0.0560	0.0020	38.8	1.0	0.0256	0.0006	163	4	Oscillatory
*TAS21-22.1	492	337	0.68	14	0.01	0.0480	0.0010	37.9	0.8	0.0265	0.0006	168	3	Cloudy
*TAS21-16.1	88	61	0.69	2	4.6	0.0910	0.0040	38.0	1.0	0.0249	0.0007	159	5	(Oscillatory)
TAS21-22.2	61	90	1.49	2	2.9	0.0750	0.0040	46.0	2.0	0.0213	0.0007	136	5	Unzoned rim
*TAS24-12.2	418	1552	3.71	21	1.6	0.0640	0.0020	37.9	0.8	0.0260	0.0005	165	3	Oscillatory
*TAS24-19.1	119	712	5.99	8	1.1	0.0590	0.0030	37.6	1.0	0.0263	0.0007	167	4	Unzoned rim
TAS24-17.1	1257	488	0.39	21	0.20	0.0500	0.0010	61.0	2.0	0.0163	0.0006	104	4	Altered rim
TAS24-17.2	916	117	0.13	14	0.40	0.0520	0.0010	64.0	1.0	0.0156	0.0003	100	2	Altered rim
TAS24-19.2	203	971	4.80	12	1.0	0.0580	0.0020	41.0	1.0	0.0244	0.0007	155	4	Altered
TAS24-14.1	144	1387	10.0	11	1.7	0.0650	0.0030	43.0	1.0	0.0231	0.0006	147	4	Unzoned rim
TAS24-12.1	1559	471	0.30	35	0.51	0.0536	0.0007	44.5	0.9	0.0224	0.0004	143	3	Altered rim
TAS25-1.1	146	165	1.12	4	4.6	0.0910	0.0040	41.0	1.0	0.0230	0.0006	147	4	Light rim
TAS25-13.1	138	88	0.64	3	4.1	0.0860	0.0040	44.0	1.0	0.0217	0.0007	139	4	Light rim

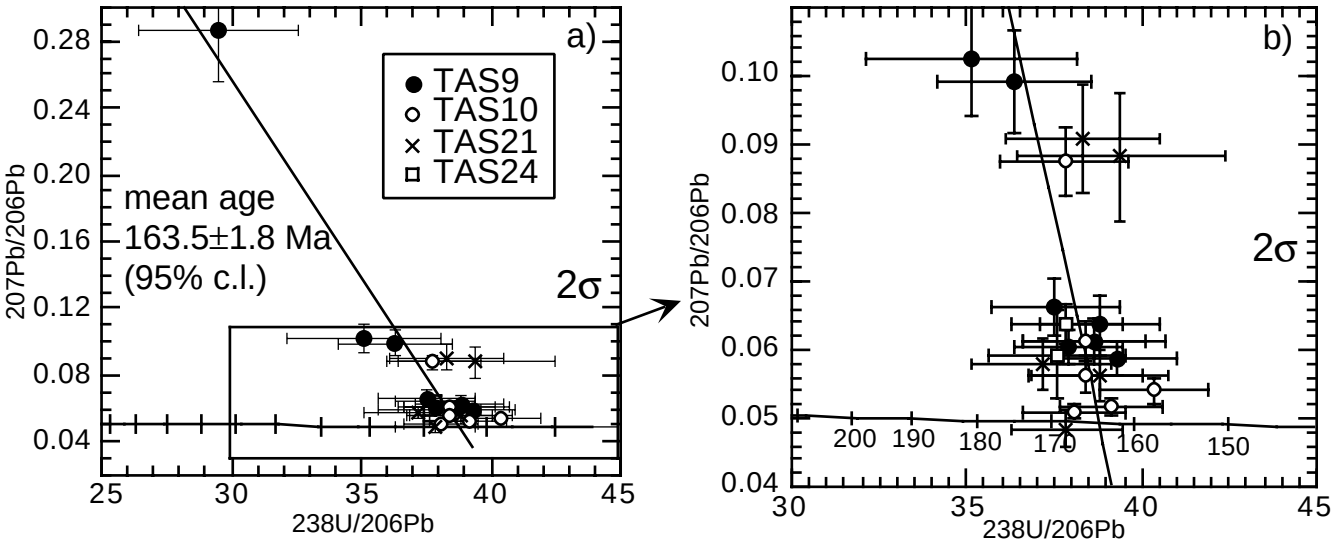

Fig. 7 Mellichen metagabbro: TW diagram. Only the analyses yielding the Jurassic intrusion age are plotted

collected, inherited zircons were found (Table 7). In one sample from the Allalin gabbro (MAT6), in a low-grade vein from the Täsch Valley (TAS2) and in one of the LdC eclogites (CIG1) the zircons are exclusively inherited. Most of these zircons display different CL-patterns cross cutting each other and are overgrown by magmatic zircon of Jurassic age, as expected for inherited zircon in a magmatic rock.

As most of the data give relatively old ages, they were corrected for common lead using the measured ^{204}Pb and were plotted on a conventional Wetherill concordia diagram (Fig. 13a, b). Although most of the zircons were affected by lead loss and are therefore discordant, the following conclusions may be drawn: (1) Precambrian components are present in particular in the Allalin gabbro. (2) Some data points from the eclogite CIG1 are around 450 Ma. They are very close to concordia and therefore their ages, even if not correct, likely argue for Ordovician or Cambrian components. (3) Several inherited zircons from the Allalin gabbro yielded Carboniferous ages. When these data are plotted on a TW diagram (Fig. 13c) three data points around 336 Ma lie on a mixing line between the radiogenic end member and common Pb. The discordance on the conventional concordia diagram may be due to the analytical imprecision of the ^{204}Pb common lead correction. (4) In the low-grade vein from the Täsch Valley two data points around 287 Ma are concordant (Table 7 and Fig. 13a). However, concordance is not necessarily evidence of geological significance. It cannot be excluded that the 287 Ma ages could be due to partial lead loss from an original older Pb component.

In the gabbroic samples from the Täsch Valley ca. 30% of the analyses yield ages that scatter between the Jurassic formation age and the Eocene (Table 4). As these data points do not form a cluster about a common age, they are not considered to reflect geologically meaningful events. Rather they are interpreted to represent radiogenic lead loss during the Alpine H*P* metamorphism. Interestingly, no ages younger than 44 Ma have been detected thus far excluding any lead loss after the Middle Eocene event.

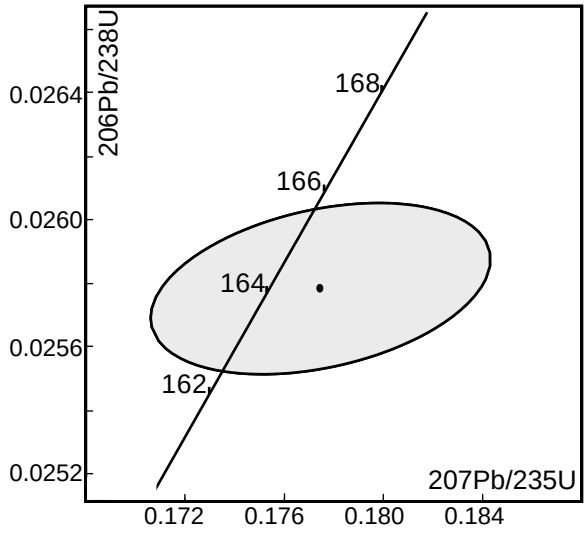

U (ppm)	Th/U	Pb rad (ppm)	206/204
66.8	1.7	2.4	206
	206/238	**207/235**	**207/206**
	0.02578 ±0.00011	0.17747 ±0.00280	0.04992 ±0.00074
Age (Ma)	164.1±0.7	165.9±3.1	191.4±34.2

Fig. 8 Metagabbro TAS21: concordia diagram for conventional isotope dilution analysis. The ^{206}Pb/^{238}U age is in agreement with the age obtained with SHRIMP

6 Discussion and interpretation

6.1 The Jurassic intrusion ages

In both the ophiolitic metagabbros investigated the zircons show mainly magmatic oscillatory zoning and have U-contents as well as Th/U ratios typical for magmatic crystals. These two gabbros yielded indistinguishable ages of 164.0 ± 2.7 Ma and 163.5 ± 1.8 Ma, indicating that the ophiolitic gabbros intruded in the Middle Jurassic.

These data represent the most precise dating of the formation of the ophiolites in the Zermatt–Saas-Fee area. The formation age of the Zermatt–Saas-Fee mafic sequence so far was indirectly dated by the stratigraphy of the overlying sediments. Previous attempts to date these ophiolites used K/Ar on blue amphiboles and phengites (Bocquet et al. 1974; Delaloye and Desmons 1976). The ages obtained either had no geological significance or very large errors.

The protolith ages obtained for these ophiolitic gabbros are in line with data from other ophiolites belonging to the Tethys ocean. In the Ligurian Alps (southernmost portion of the Piemontese–Ligurian ocean) and Northern Apennines, zircon data yielded in part concordant ages between 150 and 156 Ma for the opening of the ocean (Borsi et al. 1996). Ages similar to those of the ZSFO were obtained for another ophiolitic slice tectonically emplaced in a more external position of the Alpine edifice (Gets nappe). Gabbros yielded U-Pb ages of zircons at 166 ± 1 Ma and an amphibole $^{40}Ar/^{39}Ar$ plateau age of 165.9 ± 2.2 Ma (Bill et al. 1997). The identical ages of these ophiolites and the ZSFO confirm the hypothesis that they originated from the Piemontese–Ligurian ocean. Of more difficult interpretation are the Sm-Nd and U-Pb data (Costa and Caby 1997) on a slice derived from the Piemontese–Ligurian ocean that escaped intensive Alpine deformation (Montgenèvre ophiolites). The authors interpreted these data as indicating crystallization of gabbros at 185 ± 22 Ma (Sm–Nd on whole rock) and later intrusions of a diorite at ca. 160–155 Ma (U-Pb on zircon). Such a supposedly ''long-lived oceanization'' is not confirmed by our data. In the ZSFO the crystallization ages of the Allalin gabbro and of more differentiated magma of the Mellichen leucogabbros are indistinguishable.

6.2 The deposition age of the ophiolitic sediments

In sedimentary rocks the magmatic age of the youngest detrital zircon gives a maximum depositional age. In both the metasediments at Sparrenflue and at LdC, zircon cores yielded Late Jurassic ages. The most reliable age is the 161 ± 11 Ma obtained with three concordant data points within the same zircon core. As the three data points give the same age the possibility of uniform radiogenic lead loss is very unlikely. In the case of the Mn-metaquartzite at Sparrenflue the two youngest ages are around 153–154 Ma and, although they are single data from single cores, they are in tune with a maximum Late Jurassic deposition age of the oceanic sediments. This age is in agreement with biostratigraphic arguments that indicate a Middle to Late Jurassic age for the deposition of the radiolarites in the Tethys (e.g. Baumgartner 1987).

The presence of euhedral, relatively large (200–300 μm) detrital zircons of various ages in the meta-

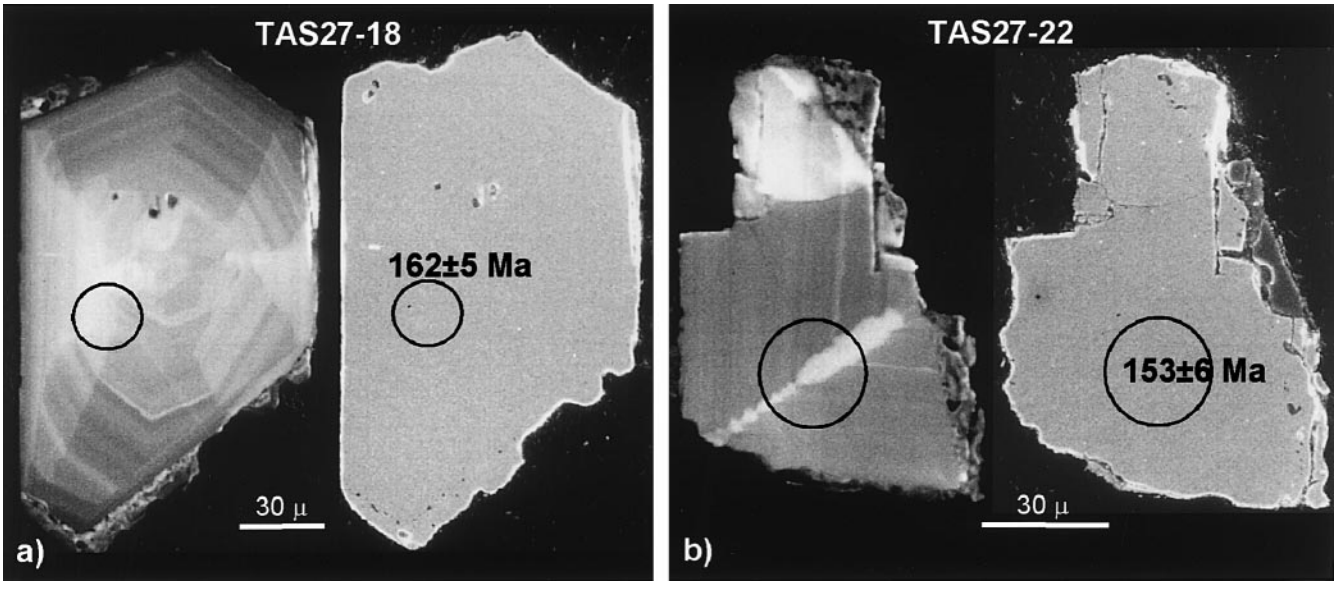

Fig. 9a, b Zircons from the Mn-metaquartzite at Sparrenflue (TAS27): secondary electron images (on the *right*) and panchromatic CL images (on the *left*). Note that the oscillatory zoning is similar to that of the zircons from the metagabbros (Figs. 4 and 6). **a** TAS27-18: zircon with a magmatic oscillatory zoning preserving its original euhedral shape, **b** TAS27-22: zircon that yields the youngest ages

Table 5 Metasediment at Sparrenflue (TAS27): U, Th and Pb SHRIMP data

Spot name	U (ppm)	Th (ppm)	Th/U	Pb radiogenic (ppm)	% Common Pb	207/206 uncorrected	± 207/206	238/206 uncorrected	± 238/206	206/238	± 206/238	Age (Ma) 206/238	±	CL domain
TAS27-23.1	154	100	0.65	4	7.8	0.1210	0.0050	33.9	0.9	0.0272	0.0008	173	5	Oscillatory
TAS27-18.1	51	23	0.46	1	11	0.1520	0.0060	34.9	1.2	0.0254	0.0009	162	5	Oscillatory
TAS27-19.1	92	42	0.45	3	18	0.2160	0.0080	30.9	0.9	0.0265	0.0008	168	5	Oscillatory
TAS27-11.1	400	860	2.15	11	6.0	0.1030	0.0030	38.8	0.9	0.0242	0.0006	154	4	Oscillatory
TAS27-14.1	559	613	1.10	18	3.4	0.0800	0.0010	36.0	0.8	0.0268	0.0006	171	4	Oscillatory
TAS27-15.1	322	140	0.43	8	5.4	0.0990	0.0030	37.5	0.9	0.0252	0.0006	161	4	Oscillatory
TAS27-22.1	47	22	0.46	1	14	0.1750	0.0100	35.9	1.2	0.0240	0.0009	153	6	Oscillatory

sediment CIG3, which overlay the metabasalts, suggests a detrital influx from a nearby continent. The proximity of a continent would imply that the ZSFO do not represent a classical Mid-Ocean-Ridge sequence, but that they formed in a relatively small basin or close to a continental margin.

Another important point arises from the similar ages of all the zircons dated from the Mn-metaquartzite TAS27. This sample is an uncommon metasediment, as one may have expected a more heterogeneous age range for a detrital population. As deposition of sediments is a low temperature process, there is no reason to believe that the U-Pb system of the zircons contained in the Mn-sediment were all reset in Jurassic time during deposition. Therefore, these ages indicate that the source of the sedimentary zircons is of Jurassic age. Similar shape, zonation, U-contents, Th/U ratios and age of the zircons extracted from this Mn-sediment and from the metagabbros of the ophiolitic sequence argue for a provenance of the detrital zircons from these gabbros. Moreover, the preservation of euhedral zircon shapes implies that their deposition did not occur after a long transport. Tectonic brecciation and intra-oceanic erosion would be likely processes by which zircons from the ophiolitic gabbros could have been deposited in a short time and with little transport into the marine sediments. The same logic applies for the euhedral core of Late Jurassic age found in a detrital zircon from the LdC metasediments (Fig. 10a).

In conclusion, the Mn-metaquartzites were deposited on top of the mafic rocks in the Late Jurassic. It is likely that submarine extensional tectonics followed by submarine erosion accompanied their deposition.

6.3 Inherited zircons

The inherited zircons within the metagabbros and metabasalts yielded the age of well known magmatic cycles documented in the Alpine poly-metamorphic continental crust, in particular the Carboniferous and the Permian ages (Gebauer 1993). Therefore, it is likely that the source of the basic magmas was contaminated by subduction of a continental crust. However, if the ages of Permian zircons found in the quartz–zoisite vein within metabasalts (TAS2) are geologically significant, at least part of the zircons was not carried down to the magma source by subducting continental slab, because in the Alps no subduction occurred between the Permian and the Jurassic. An alternative hypotheses for the origin of Permian zircon components in the ophiolitic metabasalts is that the Permian zircons found in the vein were assimilated into the basalts when the magmas intruded sediments at the ocean floor, which can contain detrital zircons (section 5.5.). The zircons were then transferred into the metamorphic vein during Alpine metamorphism.

Although the interpretation that these zircons were once part of sediments is preferred, the possibility that

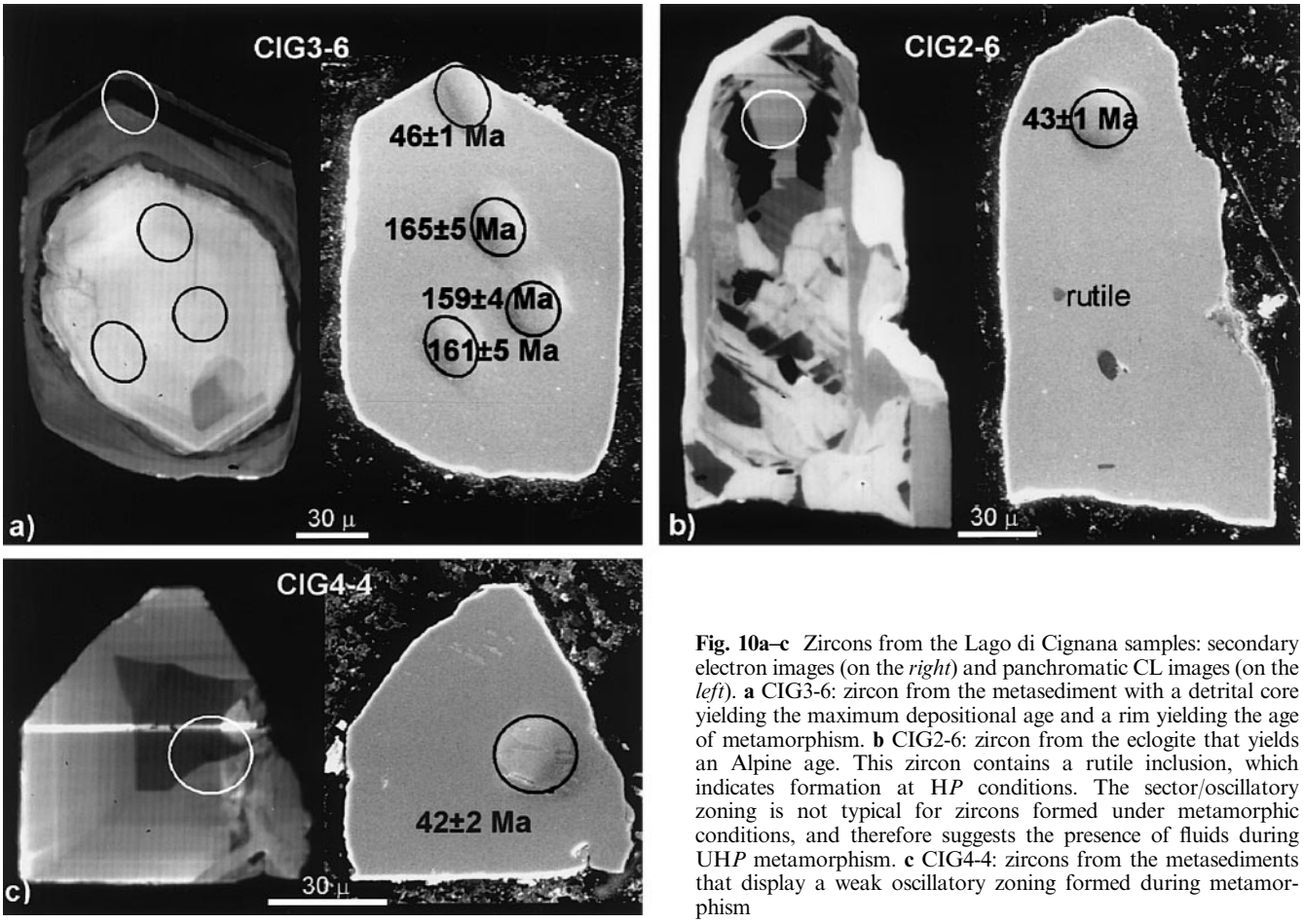

Fig. 10a–c Zircons from the Lago di Cignana samples: secondary electron images (on the *right*) and panchromatic CL images (on the *left*). **a** CIG3-6: zircon from the metasediment with a detrital core yielding the maximum depositional age and a rim yielding the age of metamorphism. **b** CIG2-6: zircon from the eclogite that yields an Alpine age. This zircon contains a rutile inclusion, which indicates formation at H*P* conditions. The sector/oscillatory zoning is not typical for zircons formed under metamorphic conditions, and therefore suggests the presence of fluids during UH*P* metamorphism. **c** CIG4-4: zircons from the metasediments that display a weak oscillatory zoning formed during metamorphism

they crystallized in the mantle and were carried up by the mafic melts cannot be ruled out. This hypothesis would imply that the zircons formed at different times and remained trapped in the mantle until the Jurassic.

6.4 The age of Alpine metamorphism

The 15 data points of the LdC samples that cluster at 44.1 ± 0.7 Ma indicate that the zircons within eclogites and metasediments of the ZSFO recorded a geological event in the Middle Eocene. During Alpine convergence the ZSFO underwent subduction and exhumation and the age of 44.1 ± 0.7 Ma must necessarily date an event in this evolution.

Most of the zircons that yielded the Eocene age have low Th/U ratios, generally below 0.1, as typically observed in metamorphic zircon domains (e.g. Claesson 1987; Williams and Claesson 1987; Pidgeon 1992; Collins and Williams 1995; Gebauer 1996; Gebauer et al. 1997; Rubatto and Gebauer in press). The absence of any inherited cores in the zircons of the eclogite CIG2 and the metasediment CIG4 and the presence of a rutile inclusion indicate that the zircons are not the products of recrystallization of previous magmatic crystals. It is proposed that, during metamorphism, new zircon either overgrew previous detrital cores (Fig. 10a) or completely newly crystallized (Fig. 10b and c). New metamorphic zircon formation is also suggested by the regular and homogeneous zoning of the crystals, not common in crystals with a poly-episodic history. On the other hand, zircons that did not record the Eocene event, may have been protected as inclusions in stable minerals.

The zircons that yield an Eocene age display oscillatory zoning, which is typical for crystals grown in equilibrium with a melt or a fluid (Rubatto and Gebauer in press). Therefore, it is further suggested that they formed in the presence of metamorphic fluids, which have been documented by Reinecke (1991) and van der Klauw et al. (1997). The possibility of crystallisation from a melt is ruled out by the absence of partial melting or intrusions during the Alpine history of the ZSFO, by the low Th/U ratios of the Eocene zircon domains and by the rutile inclusion.

The *P-T* evolution of the LdC rocks (Reinecke 1991; Reinecke 1995; van der Klauw et al. 1997) shows progressive increase in pressure and temperature that led to a metamorphic peak of 580–630 °C and ca. 28 kbar. The maximum pressure of 28–30 kbar was attained at ca. 30–45 °C lower temperature than the thermal peak. At these conditions coesite was stable in eclogites and metasedi-

Table 6 Lago di Cignana samples (CIG2, CIG3 and CIG4): U, Th and Pb SHRIMP data ($^{+}$ indicates the data of Eocene age that were considered for the calculation of the age of metamorphism). When the CL zonation pattern is given in *brackets* the zoning is not well defined (* indicates zircon cores)

Spot name	U (ppm)	Th (ppm)	Th/U	Pb radiogenic (ppm)	% Common Pb	207/206 uncorrected	±207/206	238/206 uncorrected	±238/206	206/238	±206/238	Age (Ma) 206/238	±	CL domain
$^{+}$CIG2-2.1	273	2	0.01	2	0.90	0.0550	0.0020	142	3	0.0070	0.0002	44.8	1.0	Unzoned
$^{+}$CIG2-4.1	278	2	0.01	2	0.60	0.0520	0.0020	140	3	0.0071	0.0002	45.5	0.9	Sector
$^{+}$CIG2-6.1	426	4	0.01	3	0.80	0.0550	0.0020	147	3	0.0068	0.0001	43.4	0.8	Sector
$^{+}$CIG3-1.1	166	< 1	< 0.01	1	1.9	0.0640	0.0030	144	3	0.0068	0.0002	43.7	1.1	Sector
$^{+}$CIG3-1.2	9	1	0.11	0	37	0.3900	0.0400	91.0	11.0	0.0069	0.0009	44.6	6.0	Sector
$^{+}$CIG3-3.1	21	< 1	0.02	0	11	0.1400	0.0200	147	10	0.0061	0.0004	39.1	2.8	Light rim
$^{+}$CIG3-3.2	44	11	0.25	0	22	0.2500	0.0200	124	8	0.0063	0.0004	40.2	2.7	Oscillatory*
$^{+}$CIG3-5.1	64	1	0.01	0	3.1	0.0750	0.0040	152	5	0.0064	0.0002	41.1	1.3	Unzoned rim
$^{+}$CIG3-5.2	44	6	0.14	0	8.0	0.1230	0.0080	137	5	0.0067	0.0003	43.0	1.7	Oscillatory*
$^{+}$CIG3-11.1	17	28	1.6	0	10	0.1400	0.0100	121	7	0.0074	0.0004	47.5	2.8	Oscillatory*
$^{+}$CIG3-8.1	121	1	0.01	1	2.1	0.0660	0.0030	148	4	0.0066	0.0002	42.5	1.1	Unzoned rim
$^{+}$CIG3-9.1	335	1	< 0.01	2	1.3	0.0590	0.0020	137	3	0.0072	0.0001	46.3	0.9	Oscillatory
$^{+}$CIG3-6.2	221	1	< 0.01	1	1.3	0.0590	0.0020	138	3	0.0072	0.0002	46.0	1.1	(Oscillatory)
CIG3-6.1	58	46	0.80	2	1.4	0.0620	0.0020	39.4	0.9	0.0251	0.0006	159	4	Oscillatory*
CIG3-6.3	56	33	0.59	2	1.6	0.0640	0.0030	38.0	1.0	0.0259	0.0008	165	5	Oscillatory*
CIG3-6.4	66	47	0.72	2	1.8	0.0660	0.0020	39.0	1.0	0.0252	0.0007	161	5	Oscillatory*
CIG3-2.2	200	79	0.40	57	0.85	0.1009	0.0007	3.59	0.06	0.2760	0.0050	1571	23	Oscillatory*
CIG3-13.1	284	68	0.24	19	0.45	0.0595	0.0007	14.4	0.2	0.0690	0.0010	432	7	Oscillatory
CIG3-8.2	527	220	0.42	22	0.36	0.0546	0.0007	24.4	0.4	0.0409	0.0007	258	4	Oscillatory*
CIG3-8.3	572	191	0.33	21	0.32	0.0537	0.0006	27.5	0.4	0.0362	0.0006	229	4	(Oscillatory)*
CIG3-2.1	186	6	0.03	6	2.9	0.0770	0.0010	26.6	0.5	0.0366	0.0006	231	4	Unzoned
$^{+}$CIG4-4.1	27	30	1.1	0	11	0.1500	0.0100	137	7	0.0065	0.0003	41.7	2.2	Oscillatory
$^{+}$CIG4-6.1	4	2	0.44	0	38	0.4000	0.0500	104	11	0.0059	0.0008	38.1	5.4	Oscillatory

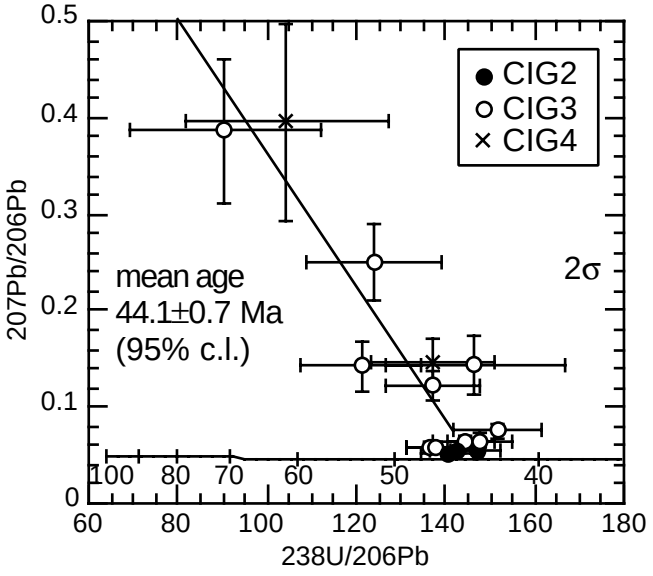

Fig. 11 Lago di Cignana samples: TW diagram for the Eocene data, which group in a well-defined cluster and are in limit of error to each of the others in 2 sigma error

ments (Reinecke 1991), indicating that the oceanic basement and its cover were subducted as a coherent unit. This stage was followed by decompression accompanied by temperature decrease down to ca. 5 kbar and 400 °C, into greenschist-facies conditions. The maximum temperature and pressure were nearly coeval and higher temperatures were not reached during decompression (Reinecke 1995). Zircon growth is generally documented at high temperature during granulite-facies metamorphism (e.g. Williams and Claesson 1987; Collins and Williams 1995; Vavra et al. 1996) or high pressure-high temperature metamorphism (Gebauer 1996). It is proposed that zircons in the LdC rocks grew around the temperature peak (600 °C), a temperature lower than in the cases mentioned above. Zircon growth

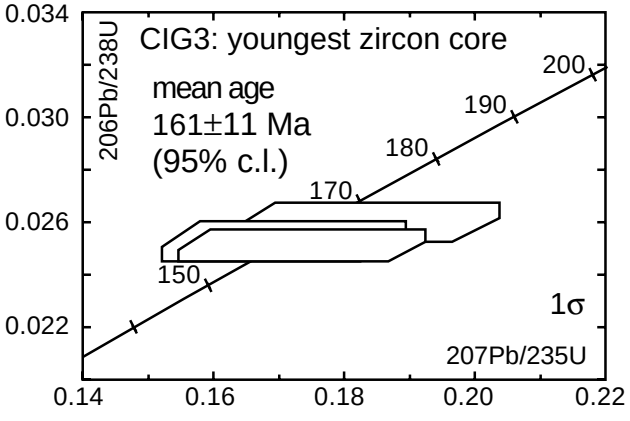

Fig. 12 Lago di Cignana metasediments (CIG3-6): concordia diagram of the youngest zircon. The three data points were obtained by SHRIMP analyses within the same zircon core. Data are shown in Table 6

Table 7 Samples TAS2, MAT6, MAT2 and CIG1: U, Th and Pb SHRIMP data for the zircons with inherited age components (* indicates $^{207}Pb/^{206}Pb$ ages). When the CL zonation pattern is given in *brackets* the zoning is not well defined

Spot name	U (ppm)	Th (ppm)	Th/U	Pb radiogenic (ppm)	% common Pb	206/238	±206/238	207/235	±207/235	207/206	±207/206	Age (Ma) 206/238	±	CL domain
TAS2-11.1	1119	397	0.36	51	0.60	0.0456	0.0007	0.3250	0.0080	0.0517	0.0001	287	4	Oscillatory
TAS2-11.2	544	245	0.45	25	0.40	0.0457	0.0007	0.3290	0.0090	0.0520	0.0010	288	5	Oscillatory
TAS2-5.1	849	185	0.22	39	0.30	0.0487	0.0008	0.3420	0.0070	0.0510	0.0006	307	5	Oscillatory
MAT6-1.1	78	87	1.1	45	0.02	0.0500	0.0100	10.50	0.20	0.1650	0.0010	*2507	10	Sector
MAT6-2.1	985	196	0.20	240	0.02	0.2450	0.0050	3.500	0.070	0.1034	0.0003	*1686	5	(Oscillatory)
MAT6-5.1	115	116	1.0	36	0.01	0.2710	0.0060	4.200	0.100	0.1114	0.0008	*1822	14	Oscillatory
MAT6-6.1	231	105	0.46	130	0.02	0.5100	0.0100	13.30	0.30	0.1900	0.0010	*2738	8	Oscillatory
MAT6-6.2	83	41	0.50	33	0.02	0.3660	0.0080	6.500	0.200	0.1290	0.0010	*2085	12	Oscillatory
MAT2-1.1	199	32	0.16	10	0.02	0.0540	0.0010	0.4200	0.0100	0.0560	0.0010	336	7	Oscillatory
MAT2-1.2	282	40	0.14	14	0.02	0.0540	0.0010	0.4000	0.0100	0.0535	0.0008	340	7	Oscillatory
MAT2-7.1	692	30	0.04	34	0.14	0.0530	0.0010	0.3900	0.0100	0.0532	0.0006	335	6	(Oscillatory)
MAT2-7.2	1479	266	0.18	69	0.01	0.0480	0.0010	0.3980	0.0080	0.0600	0.0004	303	6	(Oscillatory)
MAT2-7.3	397	138	0.35	20	0.09	0.0500	0.0010	0.3900	0.0100	0.0560	0.0010	315	6	(Oscillatory)
CIG1-2.1	391	149	0.38	41	0.10	0.1040	0.0020	0.8700	0.0200	0.0612	0.0008	635	9	Oscillatory
CIG1-2.2	328	58	0.18	25	0.40	0.0810	0.0010	0.6000	0.0200	0.0540	0.0010	502	8	Oscillatory rim
CIG1-3.1	172	22	0.13	12	0.40	0.0730	0.0010	0.5400	0.0200	0.0540	0.0020	451	7	(Oscillatory)
CIG1-1.1	164	25	0.15	11	0.02	0.0720	0.0010	0.5800	0.0100	0.0579	0.0008	450	8	Oscillatory rim
CIG1-1.2	538	131	0.24	135	0.02	0.2390	0.0050	5.000	0.200	0.1510	0.0050	*2353	51	(Oscillatory)

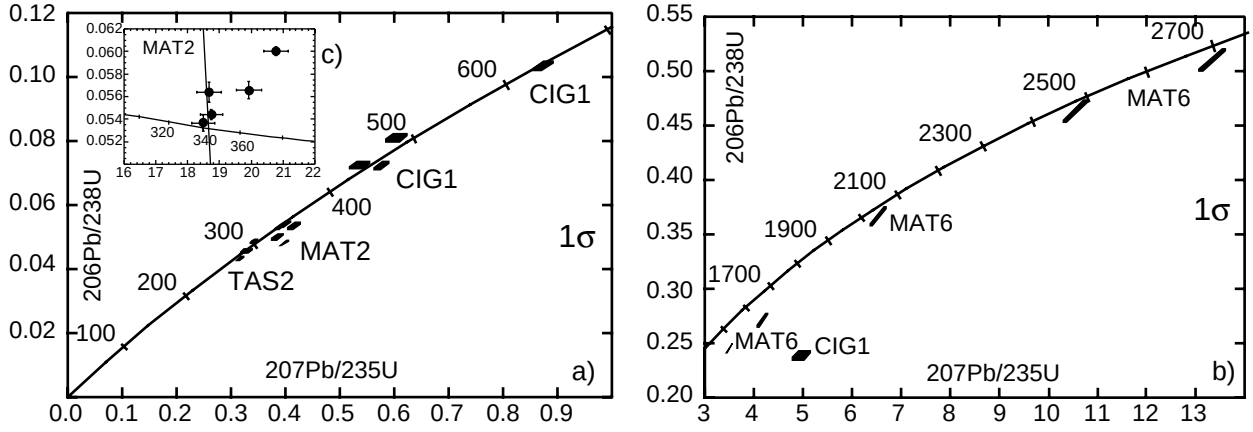

Fig. 13a–c Samples TAS2, MAT6, MAT2 and CIG1: **a** and **b** concordia diagrams for two age intervals showing the inherited age components; **c** TW diagram for the Carboniferous data points of the sample MAT2

at lower temperatures has been reported only in the case of hydrothermal veins (Rubatto et al. 1997). Moreover, the rutile inclusion in an Eocene zircon from the metasediment CIG2 supports a (U)H*P* origin of the zircon. Therefore, the 44.1 ± 0.7 Ma is interpreted as the age of UH*P* metamorphism in the LdC unit.

In the Mellichen metagabbro the age of the H*P* metamorphism could not be constrained. Most of the zircon rims of possible metamorphic origin had, as in the case of the metagabbro TAS25, too low U and radiogenic Pb-contents to be dated. However, the youngest age of the zircon rims affected by lead loss gives a maximum age for this event. The two youngest data from the leucogabbro TAS9 indicate an age of 48.8 ± 2.9 Ma and 40.3 ± 9.2 Ma, that is in agreement with the age obtained at LdC.

The Alpine subduction event in the Western Alps was believed to be of Cretaceous age (e.g. see the summary paper by Hunziker et al. 1992). However, other recent isotopic investigations proposed a Tertiary age for the eclogitic metamorphism (e.g. Gebauer et al. 1992). The first age determination that suggested a Tertiary age also for the ZSFO was carried out on garnet using Sm-Nd (50 ± 18 Ma; Bowtell 1991; Bowtell et al. 1994). A recent attempt to date garnets in the ZSFO gave an age of 40 ± 4 Ma, in tune with the U-Pb age obtained with SHRIMP (J. Åmato, personal communication). More precise data have been obtained on phengites from retrogressed eclogites (Barnicoat et al. 1995) which yielded a Rb-Sr age of 44.6 ± 1 Ma and 42.3 ± 1.4 Ma. These data are within errors with the $^{40}Ar/^{39}Ar$ analyses on eclogitic white micas presented in the same work. These ages were interpreted as constraining either white mica growth or very rapid cooling through the blocking temperature of both isotopic systems, that in any case represent cooling to blueschist- or upper greenschist-facies conditions. The new 44.1 ± 0.7 Ma zircon age obtained at LdC is more precise than the Sm-Nd data and is most probably dating the metamorphic peak.

The geodynamic evolution of the Alpine compression can better be understood when the Eocene age obtained for the ZSFO is compared to (U-)H*P* ages recorded from other units within the Western and Central Alps. The Sesia-Lanzo Zone, representing the Adriatic continental margin of the Piemontese–Ligurian ocean, yields a H*P* age around the Cretaceous–Tertiary boundary. The precise U-Pb age on zircons (64.9 ± 1.2 Ma; Rubatto et al. 1995, 1997) and on titanite (66 ± 1 Ma; Ramsbotham et al. 1994; Inger et al. 1996) as well as the new Lu-Hf data on garnet (69.2 ± 2.7 Ma; Duchêne et al. 1997) clearly indicate a significantly older eclogite-facies metamorphism in the Sesia-Lanzo Zone (Adriatic margin) than in the ophiolites. On the other hand, the Briançonnais/European continental margin (Adula nappe, Monte Rosa and Dora Maira) underwent H*P* metamorphism only in the Late Eocene–Early Oligocene, ca. 10 Ma later than the oceanic crust (Gebauer 1996; Gebauer et al. 1997; Rubatto 1998). The difference in H*P* ages shows that Alpine subduction events propagated from the internal Adriatic margin (Sesia-Lanzo Zone) via the ZSFO to the European units (Adula, Monte Rosa and Dora Maira), roughly from SE to NW (Fig. 14). This conclusion implies subduction to the SE, as proposed in most geodynamic reconstructions of the Alpine collision and provides convincing evidence against recent models favouring a northwards subduction (Wortel et al. 1997).

As shown from the data summarised above, there is a time difference of ca. 30 Ma between the peak of the subduction-related metamorphism in the Adriatic margin (ca. 65 Ma) and the European continent (ca. 35 Ma), i.e. southern and northern margins of the Piemontese–Ligurian ocean to which the ZSFO belongs. The significant differences in H*P* ages within these units infer that Alpine subductions in the Western Alps did not involve the different units at the same time and that Alpine nappe formation was poly-episodic. Models that proposed simultaneous subduction of these units during one single event (e.g. Platt 1986; Polino et al. 1990; Avigad et al. 1993; Beaumont et al. 1996) are not supported by the

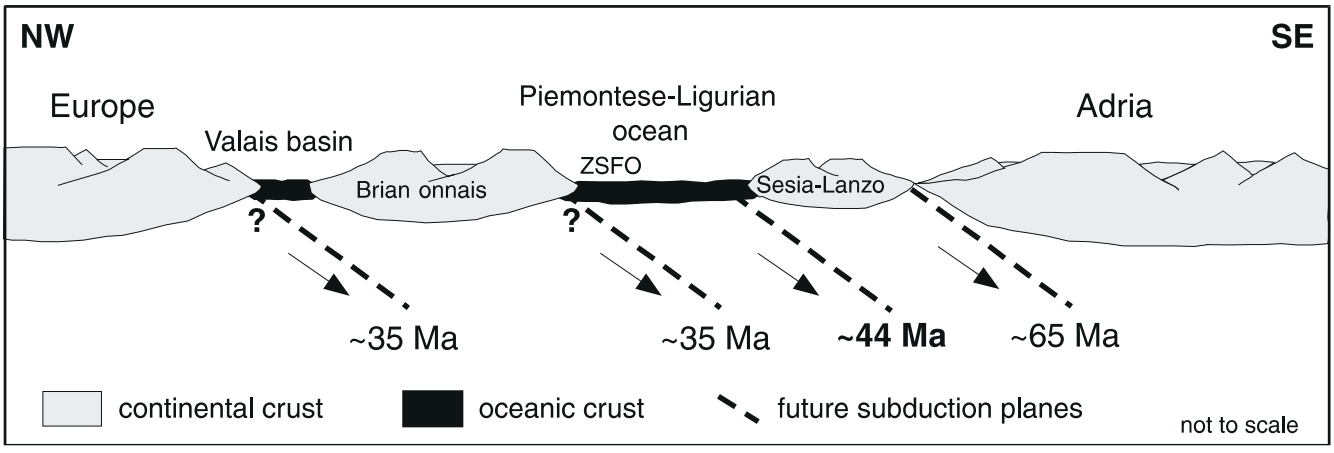

Fig. 14 Schematic paleogeographic reconstruction of the Western Alps for the Early Cretaceous with the location of the assumed future subduction zones. Different subduction episodes propagated from SE to NW involving first the Sesia-Lanzo Zone at 65 Ma, then the ZSFO around 44 Ma and finally the Briançonnais/European margin in the Late Eocene–Early Oligocene. The *question marks* indicate that the paleogeographic position of the units subducted at around 35 Ma (Adula, Dora Maira and Monte Rosa) is not certain; they could have been part of the Briançonnais or of the European continental block

geochronological data. An alternative scenario is the existence of subduction events, separated in time and paleogeographical location (Fig. 14). The Adriatic margin (Sesia-Lanzo Zone) was subducted at the Cretaceous–Tertiary boundary. As the H*P* ages suggest that the subduction was southwards, it is likely that the subduction plane was situated S of the Sesia-Lanzo Zone itself. The subduction of a relatively big slab of continental crust such as the Sesia-Lanzo Zone likely reduced the subduction rate and eventually stopped it and exhumation started in this area of the Alpine belt. Later, in the Middle Eocene, a new subduction zone was active within the ocean basin and brought the ZSFO down to ca. 90 km depth. In the Later Eocene–Early Oligocene, after the closure of the Piemontese–Ligurian ocean, the southern and the northern continental margins collided. Units of the Briançonnais/European continental margin (Adula nappe, Monte Rosa and Dora Maira) were then subducted to H*P*/UH*P* conditions under the Adriatic margin. On the other hand, in the Early Oligocene more internal units of the Alpine orogen were already exhumed to upper crustal levels. The Sesia-Lanzo Zone recorded a zircon fission track age of ~33 Ma (Hurford et al. 1989) and, according to Barnicoat et al. (1995), at 35 Ma the ZSFO were cooled below ~350 °C.

7 Conclusions

1. The time for the formation of the ZSFO is constrained by the intrusion ages of the ophiolitic metagabbros: Allalin gabbro (164.0 ± 2.7 Ma) and Mellichen gabbro (163.5 ± 1.8 Ma).

2. The metasediments that directly overlie the pillow basalts were deposited shortly after the intrusion of the gabbros. The youngest detrital zircons are dated as Late Jurassic, which provides a maximum age for deposition (161 ± 11 Ma for LdC and ca. 152–153 Ma for Sparrenflue metaquartzites).

3. The ZSFO underwent (U-)H*P* metamorphism in the Middle Eocene, at around 44.1 ± 0.7 Ma. This age is indicated by the formation of zircons in the metasediments and in an eclogite at LdC, as well as by zircon rims in the Mellichen metagabbro.

4. The presence of euhedral and relatively large zircons within the ophiolitic metasediments, which are similar in internal zoning pattern and age to zircons from the ophiolitic gabbros, suggests that the detrital zircons came from the mafic rocks. Submarine extensional tectonics followed by submarine erosion would be the processes by which zircons from the gabbros were deposited within the sediments.

5. The age of the H*P* metamorphism in the Central and Western Alps decreases from the SE to the NW. This younging of the H*P* metamorphism from the Adriatic margin (Sesia-Lanzo Zone ca. 65 Ma) through the ZSFO (ca. 44 Ma) to the European continental margin (ca. 35 Ma) indicates migration of discrete Alpine subduction episodes from SE towards NW.

6. Convergence in the Western Alps was characterised by poly-episodic subduction of continental and oceanic crust during which more external units (European margin) were subducted while the internal units (Adriatic margin and Piemontese–Ligurian ocean) were already on the exhumation path.

Acknowledgements We are grateful to Roberto Compagnoni and Jürg Meyer for guiding us in the field. The SHRIMP group at the ANU in Canberra, especially I. Williams, W. Compston and A. Nutman, are cordially thanked for the assistance given during ion microprobe analyses. A special acknowledgement goes to Urs Schaltegger for supervising the isotope dilution dating. Jörg Hermann, Lourdes Sánchez Rodríguez, Berta Ordóñez Casado and Anthi Liati are especially thanked for correcting the manuscript. The accurate reviews of Simon Inger and an anonymous reviewer led to a considerable improvement of the manuscript. This research was financially supported by the Swiss National Science Foundation (Project 20-32525.91).

References

Avigad D, Chopin C, Goffé B, Michard A (1993) Tectonic model for the evolution of the western Alps. Geology 21: 659–662

Barnicoat AC (1996) Dolomite breakdown under ultra-high pressure conditions in the Allalin gabbro of SW Switzerland. EOS AGU Fall meet 77 Suppl 46: F762

Barnicoat AC, Fry N (1986) High-pressure metamorphism of the Zermatt–Saas ophiolite zone, Switzerland. J Geol Soc London 143: 607–618

Barnicoat AC, Rex DC, Guise PG, Cliff RA (1995) The timing of and nature of greenschist facies deformation and metamorphism in the upper Pennine Alps. Tectonics 14(2): 279–293

Baumgartner PO (1987) Age and genesis of Tethyan Jurassic radiolarites. Eclogae Geol Helv 80(3): 831–879

Bearth P (1967) Die Ophiolithe der Zone von Zermatt–Saas-Fee. Stämpfli and Cie, Bern

Bearth P Schwander H (1981) The post-Triassic sediments of the ophiolite zone Zermatt–Saas-Fee and the associated manganese mineralizations. Eclogae Geol Helv 74(1): 189–205

Beaumont C, Ellis S, Hamilton J, Fullsack P (1996) Mechanical model for subduction-collision tectonics of Alpine-type compressional orogens. Geology 24(8): 675–678

Bill M, Bussy F, Cosca M, Masson H, Hunziker JC (1997) High-precision U-Pb and $^{40}Ar/^{39}Ar$ dating of an Alpine ophiolite (Gets nappe, French Alps). Eclogae Geol Helv 90: 43–54

Bocquet J, Delaloye M, Hunziker JC, Krummenacher D (1974) K-Ar and Rb-Sr dating of blue amphiboles, micas and associated minerals from the Western Alps. Contrib Mineral Petrol 47: 7–26

Borsi L, Schärer U, Gaggero L, Crispini L (1996) Age, origin and geodynamic significance of plagiogranites in the lherzolites and gabbros of the Piedmont–Ligurian ocean basin. Earth Planet Sci Lett 140: 227–241

Bowtell SA (1991) Geochronological and geochemical studies of the Zermatt–Saas-Fee Ophiolite, Western Alps. PhD thesis, Univ Leeds, Leeds

Bowtell SA, Cliff RA, Barnicoat AC (1994) Sm-Nd isotopic evidence on the age of eclogitisation in the Zermatt–Saas ophiolite. J Metamorphic Geol 12: 187–196

Bucher K, Frey M (1994) Petrogenesis of metamorphic rocks. Springer Verlag, Berlin Heidelberg New York Tokyo

Claesson S (1987) Isotopic evidence for the Precambrian provenance and Caledonian metamorphism of high grade paragneisses from the Seve Nappes, Scandinavian Caledonides. I. Conventional U-Pb zircon and Sm-Nd whole rock data. Contrib Mineral Petrol 97: 196–204

Collins WJ, Williams IS (1995) SHRIMP ionprobe dating of short-lived Proterozoic tectonic cycles in the northern Arunta Inlier, central Australia. Precambrian Res 71: 69–89

Compston W, Williams IS, Kirschvink JL, Zhang Z, Ma G (1992) Zircon U-Pb ages for the Early Cambrian time-scale. J Geol Soc London 149: 171–184

Costa S, Caby R (1997) Evolution of the Ligurian Tethys in the Western Alps: REE study and Sm-Nd and U-Pb geochronology of the Montgenèvre ophiolite (Southeast of France). Terra Nova Suppl 1: 510

Dal Piaz GV, Di Battistini G, Kienast J-R, Venturelli G (1979) Manganesiferous quartzitic schists of the Piemonte ophiolite nappe in the Valsesia-Valtournanche area (Italian Western Alps). Mem Sci Geol Padova 32: 1–24

Delaloye M, Desmons J (1976) K-Ar radiometric age determination of white micas from the Piemont Zone, French-Italian Western Alps. Contrib Mineral Petrol 57: 297–303

Duchêne S, Blichert-Toft J, Luais B, Télouk P, Lardeaux J-M, Albarède F (1997) The Lu-Hf dating of garnets and the ages of the Alpine high-pressure metamorphism. Nature 387: 586–589

Fry N, Barnicoat AC (1987) The tectonic implications of the high-pressure metamorphism in the western Alps. J Geol Soc London 144: 653–659

Gebauer D (1993) The pre-Alpine evolution of the continental crust of the Central Alps – an overview. In: von Raumer JF Neubauer F (eds) Pre-Mesozoic Geology in the Alps. Springer Verlag, Berlin Heidelberg New York Tokyo, 93–117

Gebauer D (1996) A *P-T-t*-path for an (ultra?-) high-pressure ultramafic/mafic rock-association and its felsic country-rocks based on SHRIMP-dating of magmatic and metamorphic zircon domains; example: Alpe Arami (Central Swiss Alps). In: Earth processes: reading the isotopic code. Am Geophys Union, Washington DC, 309–328

Gebauer D, Grünenfelder M, Tilton G, Trommsdorff V, Schmid S (1992) The geodynamic evolution of garnet-peridotites, garnet-pyroxenites and eclogites of Alpe Arami and Cima di Gagnone (Central Alps) from Early Proterozoic to Oligocene. Schweiz Mineral Petogr Mitt 72: 107–111

Gebauer D, Schertl H-P, Brix M, Schreyer W (1997) 35 Ma old ultrahigh-pressure metamorphism and evidence for very rapid exhumation in the Dora Maira Massif, Western Alps. Lithos H*P*-Metamorphism Nat Exp 41: 5–24

Hunziker JC (1974) Rb-Sr and K-Ar age determination and the alpine tectonic history of the Western Alps. Mem Geol Mineral Univ Padova 31: 5–55

Hunziker JC, Desmon J, Hurford AJ (1992) Thirty-two years of geochronological work in the Central and Western Alps: a review on seven maps. Mem Geol Lausanne 13: 59

Hurford AJ, Flisch M, Jäger E (1989) Unravelling the thermotectonic evolution of the Alps: contribution from fission track analysis and mica dating. In: Coward M, Dietrich D, Park RG (eds) Alpine tectonics Geol Soc Spec. Publ, London, pp 369–398

Inger S, Ramsbotham W, Cliff RA, Rex DC (1996) Metamorphic evolution of the Sesia-Lanzo Zone, Western Alps: time constraints from multi-system geochronology. Contrib Mineral Petrol 126: 152–168

Krogh TE (1973) A low-contamination method for hydrothermal decomposition of zircon and extraction of U-Pb for isotopic age determinations. Geochim Cosmochim Acta 37: 637–649

Laubscher H, Bernoulli D (1982) History and deformation of the Alps. In: Mountains building processes. Hsü KJ (ed) ETH, Zürich

Marthaler M, Stampfli GM (1989) Le Schistes lustrés à ophiolites de la nappe du Tsaté: un ancien prisme d'accretion issu de la marge active apulien. Schweiz Mineral Petrogr Mitt 69: 211–216

Meyer J (1983) Mineralogie und Petrologie des Allalingabbros. PhD thesis, Basel Univ, Basel

Pidgeon RT (1992) Recrystallisation of oscillatory zoned zircon: some geochronological and petrological implications. Contrib Mineral Petrol 110: 463–472

Platt JP (1986) Dynamics of orogenic wedges and uplift of high-pressure metamorphic rocks. Geol Soc Am Bull 97: 1037–1053

Polino R, Dal Piaz GV, Gosso G (1990) Tectonic erosion at the Adria margin and accretionary processes for the Cretaceous orogeny of the Alps. Mem Soc Geol Fr Nouve Ser 156: 345–367

Ramsbotham W, Inger S, Cliff B, Rex D, Barnicoat A (1994) Time constraints on the metamorphic and structural evolution of the southern Sesia-Lanzo Zone, estern Italian Alps. Mineral Mag 58 A: 758–759

Reinecke T (1991) Very high pressure metamorphism and uplift of coesite-bearing metasediments from the Zermatt–Saas zone, Western Alps. Eur J Mineral 3: 7–17

Reinecke T (1995) Ultrahigh- and high-pressure metamorphic rocks of the Zermatt–Saas zone, Western Alps – Record of burial and exhumation paths. Bochumer Geol Geotechnol Arb 44: 152–157

Reinecke T, van der Klauw SN, Stöckhert B (1994) UH*P* metamorphic oceanic crust of the Zermatt–Saas Zone (Piemontese Zone) at Lago di Cignana, Valtournenche, Italy. In: 16th IMA Gen Meet, Pisa, Italy, pp 117–126

Rubatto D (1998) Dating of pre-Alpine magmatism, Jurassic ophiolites and Alpine subductions in the Western Alps. PhD thesis, ETH, Swiss Federal Inst Technol, Zürich

Rubatto D, Gebauer D (1998) Use of cathodoluminescence for U-Pb zircon dating by ion microprobe: some examples from the Western Alps. In: Pagel M, Barbin V, Blanc P, Ohnenstetter D (eds). Cathodoluminescence in geosciences. Springer Verlag, Berlin Heidelberg New York Tokyo (in press)

Rubatto D, Gebauer, D, Compagnoni R, Sanchez Rodriguez L (1995) A 65 Ma age for the eclogitization of continental crust at Monte Mucrone (Sesia-Lanzo Zone, Western Alps, Italy). In: 2nd Int Workshop orogenic Lherzolites Mantle Processes, Granada, pp 56–57

Rubatto D, Gebauer D, Compagnoni R (1997) Three subduction episodes in the Western Alps between uppermost Cretaceous and Upper Eocene. Terra Nova EUG9 9 Suppl 1: 489

Sartori M (1987) Structure de la zone du Combin entre les Diablons et Zermatt (Valais). Eclogae Geol Helv 80(3): 789–814

Schärer U, Kornprobst J, Beslier M-O, Boillot G, Girardeau J (1995) Gabbro and related rock emplacement crust: U-Pb geochronological and geochemical constraints for the Galicia passive margin (Spain). Earth Planet Sci Lett 130: 187–200

Stampfli GM (1996) The intra-Alpine terrain: a paleotethyan remnant in the Alpine Variscides. Eclogae Geol Helv 89(1): 13–42

Stampfli GM, Marchant RH (1997) Geodynamic evolution of the Tethyan margins of the Western Alps. In: Pfiffner OA, Lehren P, Heitzmann P, Müller S, Steck A (eds) Deep structure of the Swiss Alps results of NRP 20, Birchhäuser Verlag, Basel, pp 223–239

Tera F, Wasserburg G (1972) U-Th-Pb systematics in three Apollo 14 basalts and the problem of initial Pb in lunar rocks. Earth Planet Sci Lett 14: 281–304

van der Klauw SNGC, Reinecke T, Stöckhert B (1997) Exhumation of ultrahigh-pressure metamorphic ocean crust from Lago di Cignana, Piemontese zone, western Alps: the structural record in metabasites. Lithos H*P*-metamorphism Nat Exp 41: 79–102

Vavra G, Gebauer D, Schmidt R, Compston W (1996) Multiple zircon growth and recrystallization during polyphase Late Carboniferous to Triassic metamorphism in granulites of the Ivrea Zone (Southern Alps): an ion microprobe (SHRIMP) study. Contrib Mineral Petrol 122: 337–358

Williams IS, Claesson S (1987) Isotopic evidence for the Precambrian provenance and Caledonian metamorphism of high grade paragneisses from the Seve Nappes, Scandinavian Caledonides. II. Ion microprobe zircon U-Th-Pb. Contrib Mineral Petrol 97: 205–217

Wortel MJR, Visser RLM, Spakman W (1997) Slab detachment in the Alps and a change from northward to southward subduction Terra. Nova 9 Suppl 1: 109